Pure Appl. Geophys. 180 (2023), 1549–1571

https://doi.org/10.1007/s00024-022-03057-1

Pure and Applied Geophysics

Tsunami Occurrence 1900–2020: A Global Review, with Examples from Indonesia

Jessica A. Reid[1] and Walter D. Mooney[1]

Abstract—We present an overview of tsunami occurrences based on an analysis of a global database of tsunamis for the period 1900–2020. We evaluate the geographic and statistical distribution of various tsunami source mechanisms, high-fatality tsunamis, maximum water heights (MWHs) of tsunamis, and possible biases in the observation and recording of tsunami events. We enhance a global statistical overview with case studies from Indonesia, where tsunamis are generated from a diverse range of sources, including subduction zones, crustal faults, landslides, and volcanic islands. While 80% of global recorded tsunamis during 1900–2020 have been attributed to earthquake sources, the median MWH of earthquake tsunamis is just 0.4 m. In contrast, the median water height of landslide tsunamis is 4 m. Landslides have caused or contributed to 24% of fatal tsunamis. During 1900–2020, more tsunamis with water heights > 1 m occurred in Indonesia than in any other country. In this region fatal tsunamis are caused by subduction zone earthquakes, landslides, volcanos, and intraplate crustal earthquakes. Landslide and volcano tsunami sources, as well as coastal landforms such as narrow embayments have caused high local maximum water heights and numerous fatalities in Indonesia. Tsunami hazards are increased in this region due to the densely populated and extensive coastal zones, as well as sea level rise from polar ice melt and local subsidence. Interrelated and often extreme natural hazards in this region present both an opportunity and a need to better understand a broader range of tsunami processes.

Keywords: Tsunami, landslide tsunami, geologic hazards, Indonesia, Southeast Pacific.

1. Introduction

Tsunami research accelerated in response to devastating tsunamis that occurred in 1992 in Nicaragua and Indonesia. In the following three decades, additional tsunamis occurred that challenged the conventional assumptions for tsunami wave generation, propagation, and inundation (Kânoğlu et al., 2020; Okal, 2019). The preponderance of shallow subduction zone faulting and generation of tsunamis naturally led to an early focus on these sources. However, tsunami research has expanded to include: (1) tsunami source mechanisms other than typical subduction zone earthquakes, including crustal strike-slip and thrust fault earthquakes, subaerial and submarine landslides, volcanic eruptions and meteorological events; (2) environmental effects on tsunami wave propagation and inundation (e.g. coastal and shelf geometry); and (3) climatic effects, such as sea level rise. The expansion of tsunami research has shown that tsunami generation and propagation are more complex than previously thought. For comprehensive hazard mitigation, particularly in a time of rapid climate change, it is important that all tsunami generation and propagation mechanisms are observed and understood.

It is now recognized that landslides in particular are highly effective at generating local tsunamis (Bardet et al., 2003). In the past few decades, the contribution of submarine and subaerial landslides to tsunami wave generation has been documented in cases where local runup observations are too high to be explained by fault displacement models alone (Harbitz et al., 2014). Methods of modeling tsunamis have also expanded to describe wave generation and propagation from different source mechanisms, including landslides (Løvholt et al., 2015; Okal & Synolakis, 2004). Furthermore, increasingly sophisticated numerical modeling has been employed to study the amplification effects of shelf and coastal geometries (Grilli et al., 2012).

Indonesia and the surrounding region (Fig. 1) present an opportunity to study interrelated tsunami sources and effects, particularly those that are unaccounted for in current tsunami hazard mitigation strategies around the world. Tsunamigenic sources in

[1] Earthquake Science Center, US Geological Survey, Menlo Park, CA, USA. E-mail: jreid444@gmail.com; mooney@usgs.gov

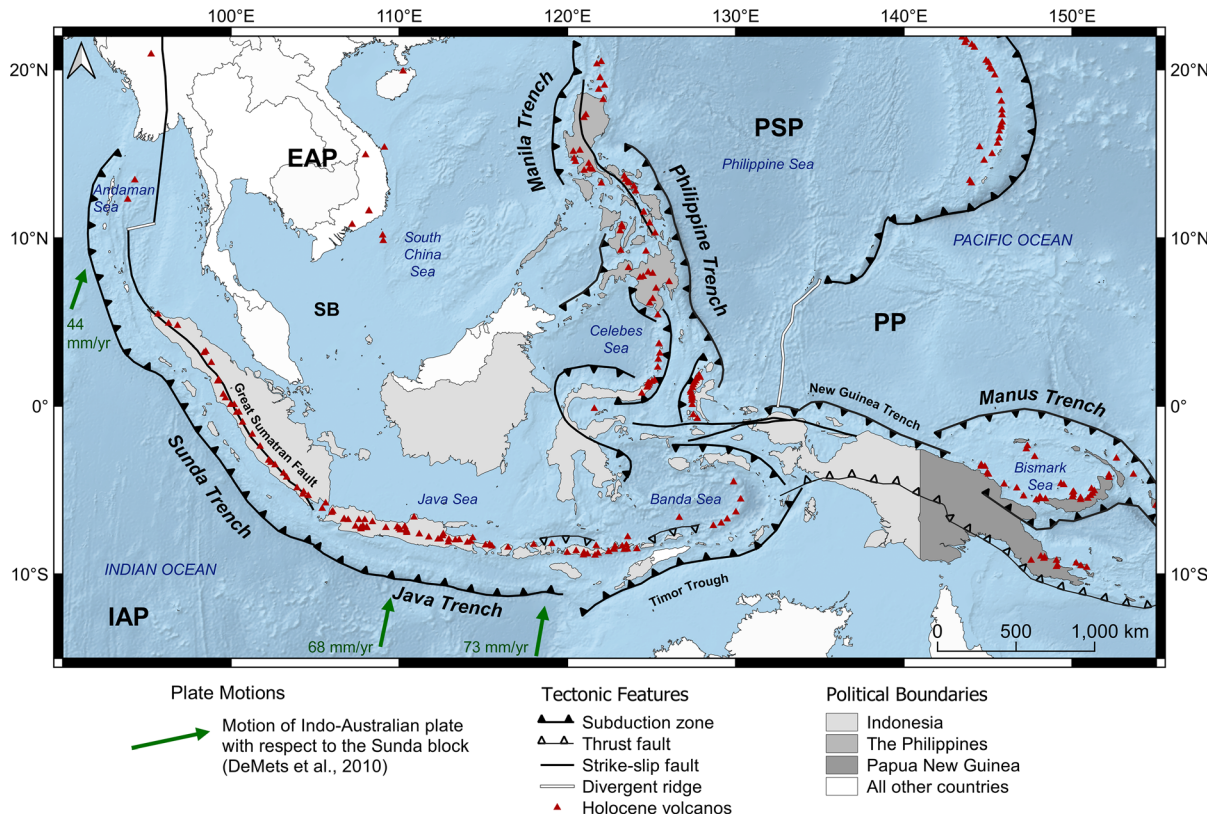

Figure 1

Simplified tectonic map of Indonesia and surrounding regions. Arc volcanism active in the Holocene is widespread. Tectonic plates are abbreviated: IAP is the Indo-Australian plate; EAP is the Eurasian plate; PSP is the Philippine Sea plate, PP is the Pacific plate, and SB is the Sunda block. Green arrows show approximate motion of the IAP with respect to the SB (DeMets et al., 2010). Of particular interest to tsunami studies are the many island and coastal volcanos. Volcano data is from Global Volcanism Program (2013). Plate boundaries and faults are modified from Bird (2003), DeMets et al. (2010), Hutchings and Mooney (2021), Hall (2012) and Cipta et al. (2016)

Indonesia are diverse, ranging from earthquakes to volcanos to landslides, often in combination (Titov, 2021). Tsunamis in this region are also extremely hazardous. In the past 120 years, seven tsunamis in Indonesia, the Philippines, and Papua New Guinea caused over 1000 fatalities each (1907, 1976, 1979, 1992, 1998, 2004, 2018) (NCEI/WDS, 2021). Four of those events involved tsunamigenic landslides (1979, 1992, 1998, 2018) (NCEI/WDS, 2021). The tsunami record of the Indonesia region demonstrates the need for assessment of local tsunami hazards, especially subaerial and submarine landslides, wave amplification effects of nearby bathymetry and landforms, and local relative sea level rise. We investigate these hazards by analyzing a compilation of global tsunami sources and effects, including maximum runups and fatalities, between 1900 and 2020. We include topographic, bathymetric and population data to study the interrelated factors of high tsunami hazard in Indonesia. Fatalities and high runups associated with various tsunami sources in Indonesia are compared to global data. We review tsunami occurrence in a diverse range of tectonic environments within Indonesia and discuss the tsunamigenic role of past and potential landslides. This work focuses on the three most common causes of tsunamis: earthquakes, volcanoes, and landslides, all of which are geologic processes. Rarer but also hazardous "meteotsunamis" are waves of comparable wavelengths to geologic tsunamis but are generated by atmospheric pressure changes. For a review of meteotsunamis, see Rabinovich (2020).

2. Data and Methods

Tsunami data recorded during 1900–2020 were obtained from the Global Historical Tsunami database maintained by the National Oceanic and Atmospheric Administration (NOAA) National Centers for Environmental Information/World Data Service (NCEI/WDS), referenced hereafter as NCEI/WDS (2021). This database contains two linked catalogs: (1) recorded tsunami events from 2100 BCE to the present, and (2) runup observations corresponding to those tsunami events. Tsunami observations including runup and water height are recorded where observed in the NCEI/WDS database. "Water height" refers to the maximum elevation in meters of the wave above a reference sea level, whereas "runup" refers to the maximum elevation in meters of ground wetted by the tsunami (NCEI/WDS, 2021). These observations are often but not always recorded at the furthest inundation point inland. While in some cases we refer specifically to runup observations, we follow the example of the NCEI/WDS database in calling the maximum observed value from a given tsunami the "maximum water height," (MWH) regardless of observation type.

An important consideration is the year when the tsunami occurred. Pre-1900 entries in the NCEI/WDS database are not comprehensive due to minimal instrumentation and inconsistent documentation of tsunami occurrence across the globe (Gusiakov, 2009). For this reason, in our statistical analyses we limit the dataset to events that occurred during 1900–2020 in order to take advantage of improved water height and earthquake monitoring technology, increased and standardized post-tsunami survey observations, and the globalization of record-keeping (Arcos et al., 2019; Synolakis & Okal, 2005). This limitation reduces the number of tsunamis we consider from 2761 to 1380 (as of December 2021; this database is dynamic and entries for past tsunamis are frequently added). While we believe that a restricted temporal range is a useful tool to reduce statistical bias, we recognize that it fails to provide the full historical context of tsunami occurrence in any given region.

We further constrain our data using "event validity" values assigned to individual events by the NCEI/WDS database. An "event validity" value indicates the likelihood that the given event was a tsunami or seiche. These values are defined as: − 1 (erroneous entry), 0 (seiche), 1 (very doubtful tsunami), 2 (questionable tsunami), 3 (probable tsunami) and 4 (definite tsunami). Our dataset only includes events with "probable" and "definite" validity designations. This limitation yields 888 tsunamis between 1900 and 2020. Limiting the year and validity fields reduces the proportion of tsunamis with unknown causes from 11 to 1%. The database also assigns the following twelve numerically coded tsunami causes, defined as: 0 (unknown); 1 (earthquake); 2 (questionable earthquake); 3 (earthquake and landslide); 4 (volcano and earthquake); 5 (volcano, earthquake and landslide); 6 (volcano); 7 (volcano and landslide); 8 (landslide); 9 (meteorological); 10 (explosion); 11 (astronomical tide). In our analyses we group codes 1 and 2 as "earthquake," codes 3 and 8 as "landslide," and codes 4, 5, 6 and 7 as "volcano."

The database has two metrics of fatalities: "deaths" and "deaths description." The latter is used in cases where a death count was not quantified, but descriptions of the event indicate that fatalities occurred. Death description categories are: "none" (0) "few" (∼ 1–50), "some" (∼ 51–100), "many" (101–1000), and "very many" (over 1000). Upon examination of fatalities associated with tsunamis, we found only 5 out of the 888 events to have no "deaths" count but a nonzero "deaths description." These tsunamis were included in the analyses involving fatalities. Events were assigned a "deaths" count equal to the minimum of the deaths description category (i.e., "few," 1 death). The total number of probable and definite tsunamis occurring 1900–2020 that caused fatalities is 127 as of December, 2021.

Population density data for Indonesia, Papua New Guinea, and the Philippines were obtained from worldpop.org. This database estimates the number of people per grid unit for 2020, adjusted to match the UN national estimates (http://esa.un.org/wpp/). Location data of active Holocene volcanoes are from the Global Volcanism Program of the Smithsonian Institution (Global Volcanism Program, 2013). All maps were generated in QGIS (QGIS, 2021).

3. Global Perspective of Fatal and High Maximum Water Height Tsunamis

3.1. Results of Global Analysis

Globally, large tsunamis occur relatively infrequently, with just 300 probable and definite tsunamis with an MWH > 1 m recorded between 1900 and 2020 (NCEI/WDS, 2021). In those 120 years, the average frequency of recorded tsunamis > 1 m is ~ 2.5/year. For the 20 year time period 2001–2020, an average of 3.4 tsunamis > 1 m were recorded each year. The interquartile range (IQR) of tsunami MWHs is 0.16–3 m. However, rare and hazardous MWHs in excess of 20 m occur more frequently in climatically or tectonically extreme regions. This includes active hotspot volcanos, modern convergent zones, and high latitudes (> 35°) (Fig. 2) in fjords, such as those in Alaska, Greenland, and Norway. Between 1900 and 2020, twenty-two tsunamis with a MWH over 20 m occurred at latitudes > 35°, compared to 5 events at latitudes < 35°.

Regions with a high concentration of tsunami occurrence are demarcated in Fig. 3a and compared in Fig. 3b. Our analysis shows that globally, 80% of tsunamis are attributed to earthquakes (Fig. 3b). 12% are caused by landslides, 5% by volcanos, 2% by meteorological events, and 1% by unknown causes. While earthquake tsunamis are more commonly observed and generally better understood, landslide and volcano tsunamis have had disproportionately large MWHs (Table 1). The median MWH observed is 3.6 m higher for landslide tsunamis than for earthquake tsunamis, whereas the median MWH for volcano tsunamis is 2.1 m higher than the median for earthquake tsunamis. Landslides cause or contribute to 23% of all tsunamis with an MWH > 1 m.

We observe that in general, fatalities are caused by tsunamis with MWHs > 1 m, and fatalities generally increase with MWH (Fig. 4). High-fatality tsunamis are geographically segregated by cause (Fig. 5a). Fatal landslide tsunamis occur at active and passive margins, frequently at high latitudes, while high-fatality earthquake tsunamis occur in active

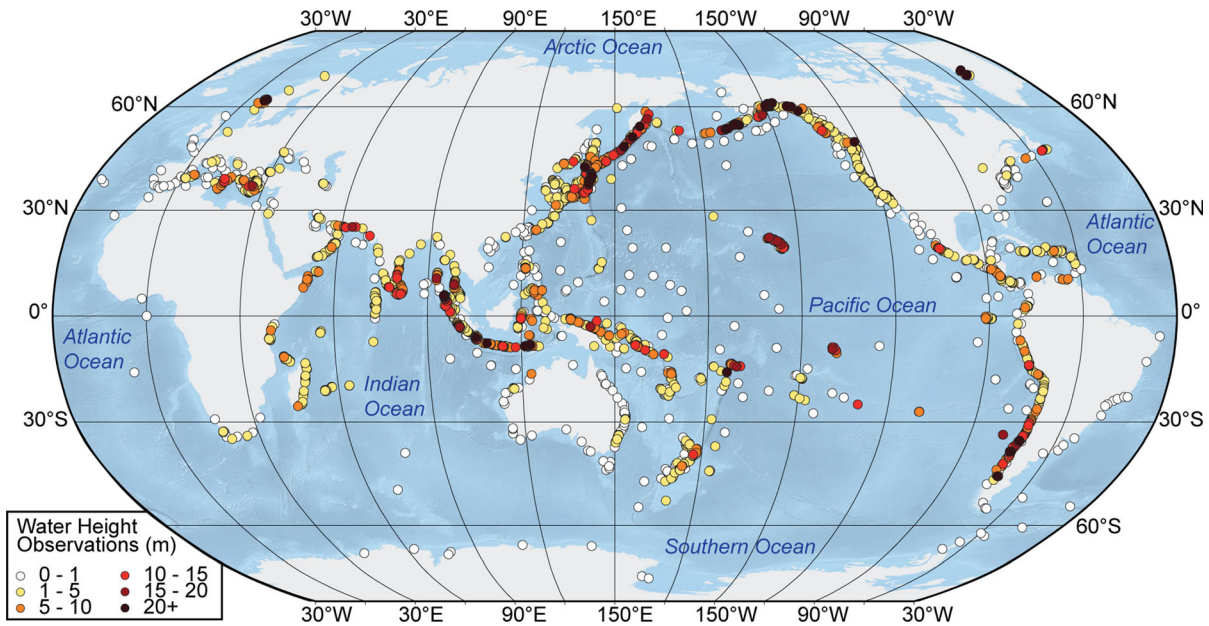

Figure 2
Global map of tsunami water height observations (1900–2020). Where observations overlap, the greatest runup values are shown. In the mid-high latitudes (> 35°), particularly in Alaska, Chile, Greenland, Norway, and Russia, water heights vary widely, with many observations > 20 m, while in the lower latitudes (35° S–35° N) water heights range more moderately from 0 to 5 m, sometimes up to 10 m. Notable exceptions include Japan, Hawaii, and Indonesia. Tsunami data are from NCEI/WDS (2021)

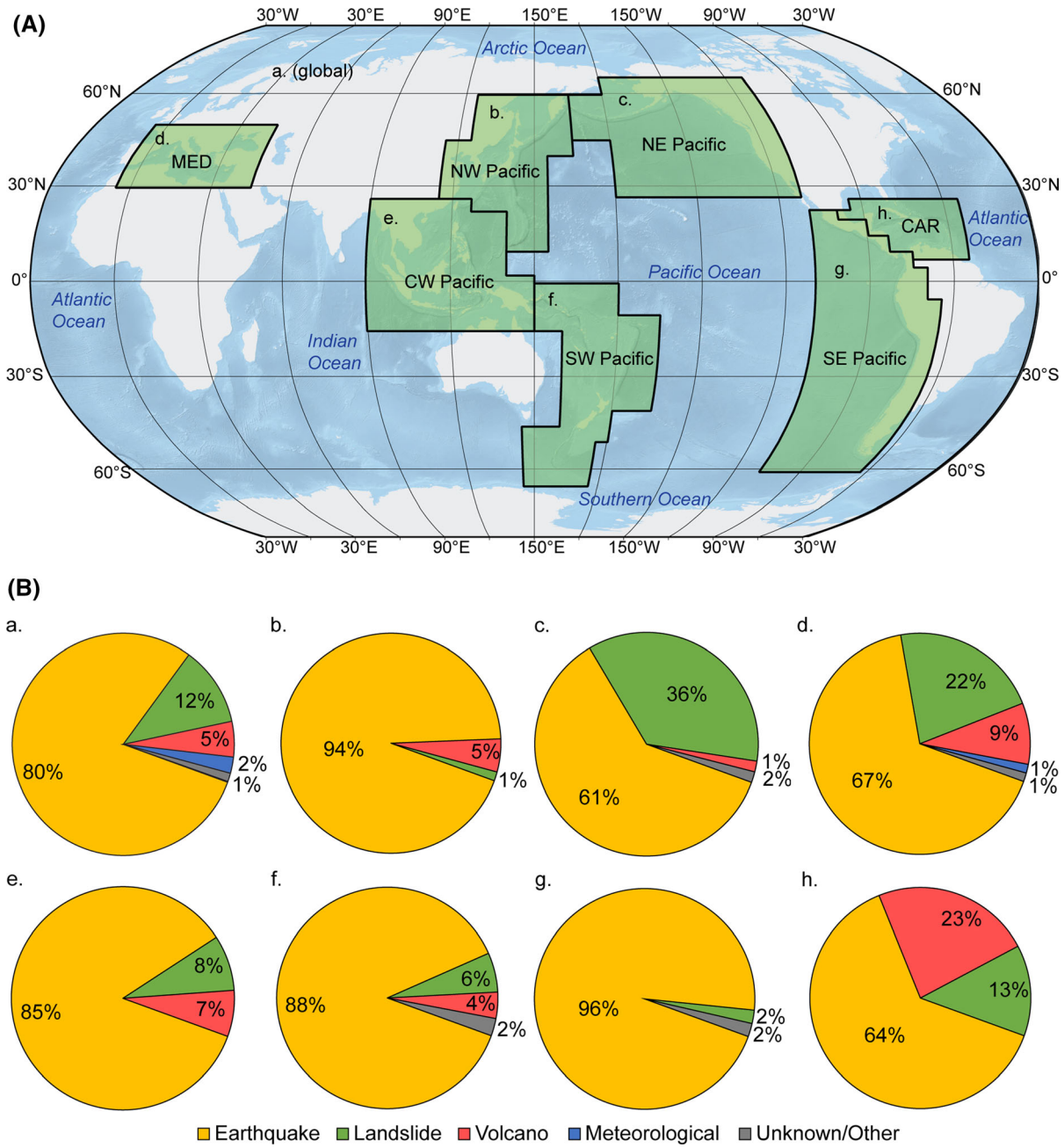

Figure 3

Distributions of tsunami causes globally and regionally (1900–2020). **a** Global distribution; **b** NW Pacific; **c** NE Pacific; **d** Mediterranean; **e** Central W Pacific; **f** SW Pacific; **g** SE Pacific; **h** Caribbean. Note the similar distributions in the Mediterranean, Caribbean, and Central W Pacific regions. Earthquakes are by far the primary cause of tsunamis in the NW Pacific and SE Pacific. Of all these regions, the NE Pacific hosts the greatest proportion of recorded landslide tsunamis. Data are from NCEI/WDS (2021)

subduction zones, most notably Japan and Central and South America. The regions of the world with fatal tsunamis attributed to volcanos, earthquakes and landslides are the Caribbean, the Mediterranean, the Philippines, Papua New Guinea, and Indonesia. Landslides, and to a lesser extent volcanos, cause

disproportionately fatal tsunamis: landslides cause or contribute to 24% of the world's *fatal* tsunamis (Fig. 5b).

3.2. Discussion of Global Observations

Our findings from Table 1 are consistent with the previous analysis of tsunami databases by Gusiakov (2020), who found that non-seismic sources (i.e., landslide, meteorological or volcanic events) caused 36.7% of tsunamis with annual maximum water heights during 1900–2020. Furthermore, despite the fact that landslide-generated tsunamis and the resulting high runups are most commonly observed in sparsely populated high-latitude regions, we confirm that landslides are particularly hazardous, causing or contributing to nearly a quarter of fatal tsunamis. Moreover, while extreme runups are often observed in high latitude fjords where the dominant geomorphic force is glacial, extreme runups may also be

Table 1

Distributions of maximum water heights (m) for tsunamis of different sources (1900–2020)

	Tsunami cause					
	Earthquake	Landslide	Volcano	Meteorological	Unknown/other	All causes
Mean	2.3	21.4	7.6	1.9	2.8	4.5
Median	0.4	4	2.5	1.7	2.4	0.6
Event Count	614	79	38	20	10	761

Data are from NCEI/WDS (2021). The above distribution includes probable and definite tsunamis (values 3 and 4) recorded globally for which a maximum water height (MWH) was recorded. The total event count of 761 is lower than the total number of probable and definite tsunamis 1900–2020 (888) because 127 such events do not have recorded water height observations in the database (92 earthquake tsunamis, 23 landslide tsunamis, 8 volcano tsunamis, 1 meteotsunami, 3 tsunamis of unknown cause). "Earthquake" includes only pure earthquake sources (cause code 1), "Landslide" includes landslide and earthquake/landslide causes (cause codes 3 and 8), "Volcano" includes all tsunamis with some volcanic element (cause codes 4, 5, 6, and 7)

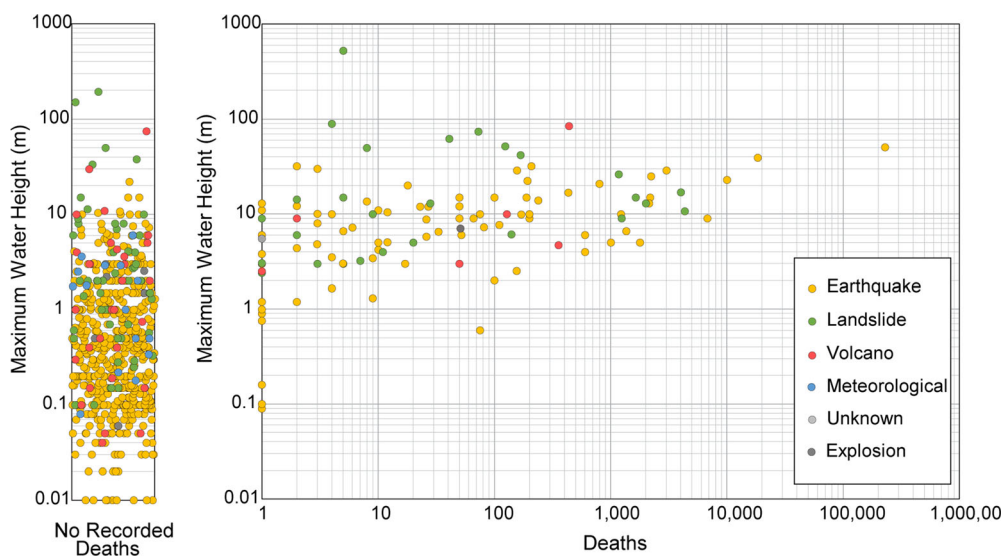

Figure 4

Global tsunamis by MWH and fatalities (1900–2020). Both axes are logarithmic. The bar on the left shows tsunamis for which no fatalities were recorded. Data are from NCEI/WDS (2021). Data points are color-coded by tsunami source. While most tsunamis cause an MWH < 1 m and no fatalities, numerous MWH > 10 m have been observed, and several tsunamis have caused over 1000 deaths. Most fatal tsunamis produce an MWH > 1 m. All fatal tsunamis with an MWH > 56 were caused largely by landslides. The volcanic source that had an MWH of 85 m and killed 437 people involved a massive flank collapse which generated the tsunami (Fig. 14)

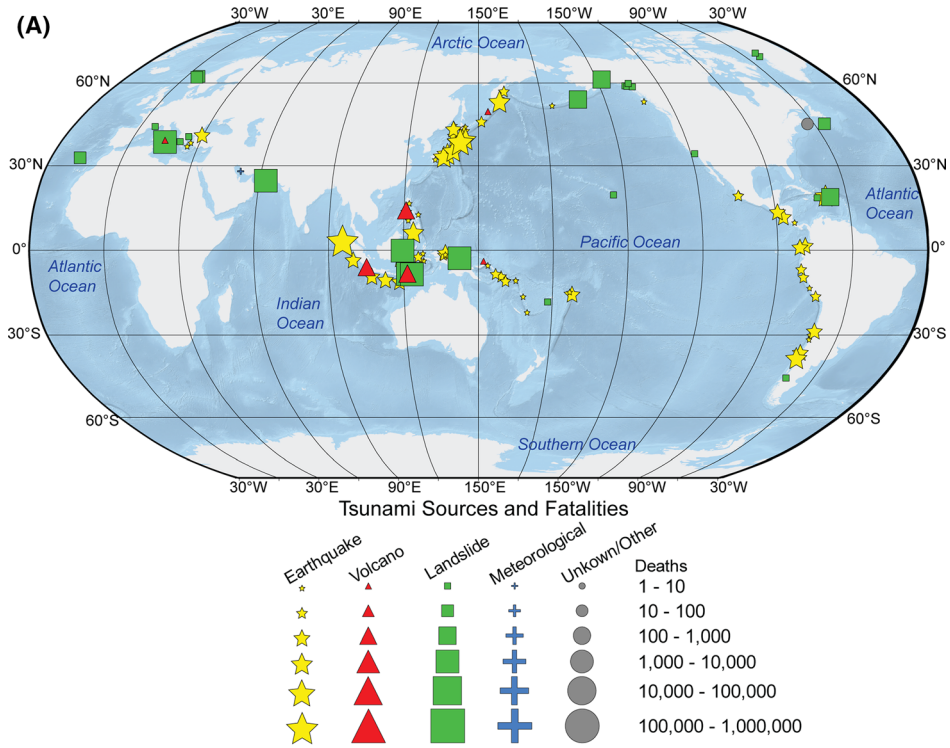

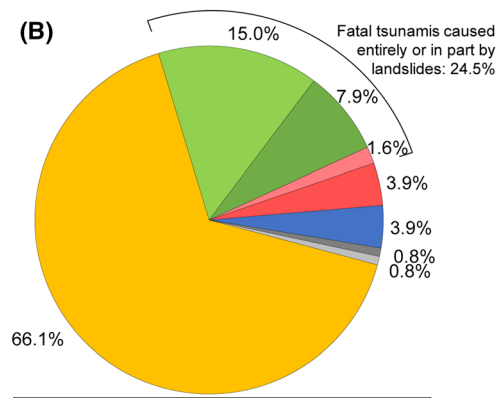

Cause Code in Database	Cause	# of events	Percent
1	Earthquake	84	66.1
3	Earthquake and Landslide	19	15.0
8	Landslide	10	7.9
7	Volcano and Landslide	2	1.6
6	Volcano	5	3.9
9	Meteorological	5	3.9
0	Unknown	1	0.8
10	Explosion	1	0.8
	Total:	127	100

Figure 5

Global distribution of fatal tsunamis by cause (1900–2020). **a** Global map of tsunamis by cause and number of deaths. Note that many fatal landslide tsunamis occur in the higher latitudes (> ∼ 35° N). Fatal earthquake tsunamis are prominent around the Pacific Ocean, as well as the northeastern Indian Ocean. Events with either a quantitative death count or a general description of nonzero fatalities are shown (127 events in total). **b** Percentage of fatal tsunamis by source mechanism. 24% of fatal tsunamis were caused at least partially by landslides. Tsunami data are from NCEI/WDS (2021)

expected in other regions where non-glacial processes have produced coastlines with similarly pronounced topography and morphology.

An important difference between earthquakes and landslides lies in the facility of observation. A submarine landslide, for example, will go unnoticed unless a significant tsunami results (and the resulting waves diverge significantly from expectations based on an earthquake source model) and an investigation follows (e.g., Tappin et al., 2001; von Huene et al., 2014). This laborious and expensive forensic practice stands in contrast to earthquake detection, which is automated. This is a possible bias in comparing the frequency of landslide versus earthquake sources; landslide tsunamis < 1 m are likely under-documented.

The coastal impact from tsunamis is fundamentally linked to climate and sea level. Thick sedimentation, unstable pore pressure, and steep subaerial and submarine morphologies have been linked to increased tsunamigenic landslides at higher latitudes, where quaternary glaciation controlled coastal processes (Twichell et al., 2009). Sea level rise also has consequences for tsunami hazard. Equatorial and tropical regions are projected to undergo more extreme storm weather and flooding in the coming decades as a result of sea level rise (Vitousek et al., 2017). These and other effects of global warming and sea level rise may affect the geographic distribution of large and deadly tsunami events and cause particular damage in low latitude regions of complex-source tsunamis.

4. *Tsunamis in Indonesia and Surrounding Regions*

The region encompassing Indonesia, Papua New Guinea, and the Philippines is a collage of island arcs, ocean basins, and continental fragments (Fig. 1; Hamilton, 1979). Four major plates are present: the Indo-Australian, Eurasian, Philippine Sea and Pacific plates (Bird, 2003; DeMets et al., 2010; Hall, 2012). Interaction between these and several micro-plates is accommodated by subduction zones, continental convergence, back-arc thrust faults, transform faults, and spreading ridges (Fig. 1; Bird, 2003; Cipta et al., 2016; DeMets et al., 2010; Hall, 2012; Hutchings & Mooney, 2021). In addition to generating volcanism and seismicity, complex tectonism constantly stretches, compresses, and shears regional landforms into intricate geometries (Hall, 2012). Many of these landforms are densely populated (Fig. 6; WorldPop, 2018), especially along coastlines.

Between 1900 and 2020, 149 tsunamis were recorded in Indonesia, Papua New Guinea, and the Philippines (NCEI/WDS, 2021). Of those events, 85% have been attributed solely to earthquakes (Fig. 3b). This result is slightly higher than the global average (80%) but is consistent with the large number of seismogenic settings in this region.

In addition to earthquake sources, since 1900 ten tsunamis partially or fully caused by volcanoes occurred in this region, accounting for 7%, which is greater than the global average of 5% (Fig. 3b). Volcanic islands are widespread here (Fig. 1) and particularly tsunamigenic due to the proximity of water. A number of these islands are densely populated (Fig. 6). Furthermore, island arcs form chains of closely arranged and vulnerable coastlines.

While only 8% of recorded tsunamis during 1900–2020 were attributed to landslides in Indonesia, Papua New Guinea, and the Philippines, many of the highest recorded water heights, and some of the highest fatality tsunamis are associated with subaerial and submarine landslides. Tsunamigenic events in this region are distributed along subduction zones, particularly the Sunda and Java trenches, but also along transform and back arc faults such as the Palu-Koro fault and the Flores thrust, respectively (Fig. 7). During 1900–2020, seven tsunamis in the Indonesian region caused over 1,000 fatalities each (Fig. 7). Of these seven, three were caused by great ($M_w \geq 8.0$) earthquakes: the 1907 Sunda trench earthquake and tsunami, the 1976 M_w 8.0 Moro Gulf earthquake and tsunami, and the 2004 M_w 9.1 Indian Ocean earthquake and tsunami (NCEI/WDS, 2021). The other four were caused fully or partially by landslides.

Earthquakes, landslides and volcanos in Indonesia and surrounding regions have produced tsunamis with runups in excess of 10–15 m (Fig. 8). In fact, between 1900 and 2020, more tsunamis with an MWH > 1 m occurred in Indonesia than in any other country, including Japan, which records tsunamis most frequently (Fig. 9). The high number of

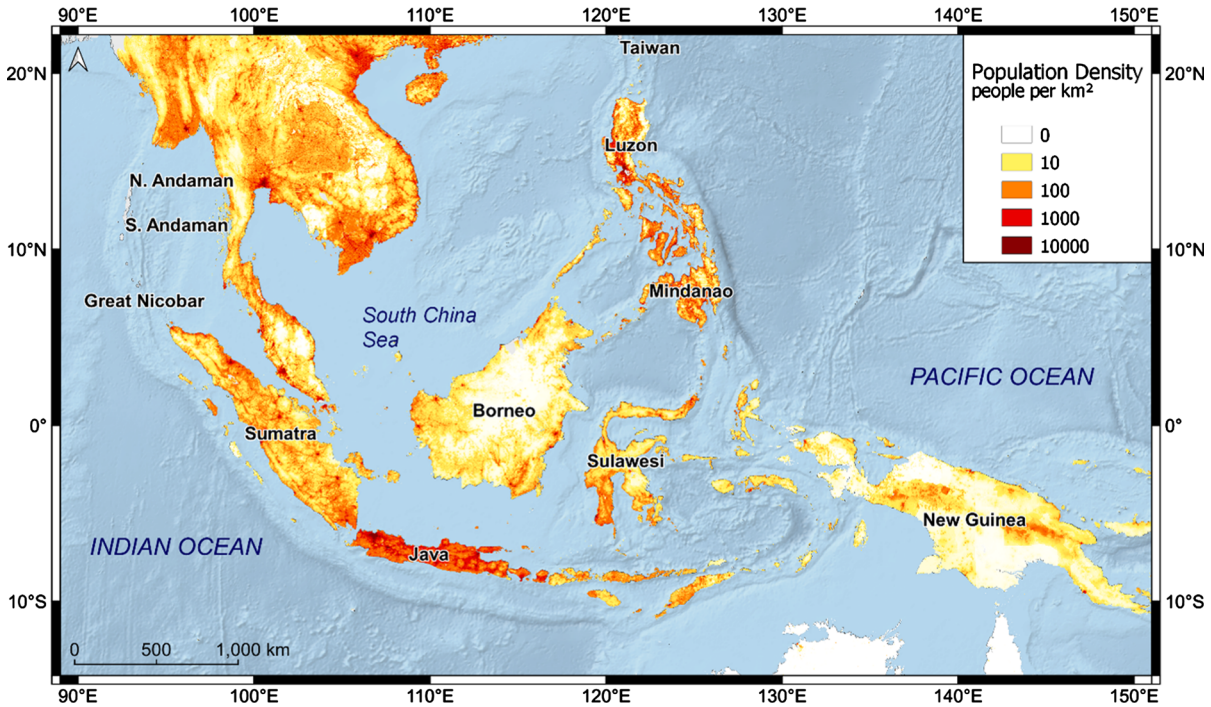

Figure 6
Map of population density. Density scale is logarithmic. Many coastal regions are densely populated, as are regions of high tsunami hazard and regions undergoing subsidence such as parts of Luzon, Java, and Sumatra. Population data is from WorldPop (2018)

tsunamis observed in Japan likely is due to extensive instrumentation, and results in a biased global distribution that does not reflect global comparative tsunami hazard. Furthermore, eight out of the twelve low-latitude (35° S–35° N) tsunamis with an MWH $\geq$ 15 m since 1900 have occurred in Indonesia. Examples of these events include: (1) the 2004 Indian Ocean 9.1 M_w earthquake (MWH: 50.9 m), (2) the 2018 Anak Krakatau volcanic eruption and flank collapse (MWH: 85 m), and (3) the 1992 Flores earthquake and landslide tsunami (MWH: 26.2 m). In such a densely populated region, high runup tsunamis cause numerous fatalities, with these particular examples causing 227899, 437, and 1169 fatalities respectively (NCEI/WDS, 2021).

5. *Indonesian Tsunamis by Tectonic Setting*

The following sections describe the tsunami history and present-day hazards in several regions of Indonesia. These regions serve as examples of different tectonic and geomorphologic environments, and the particular tsunami hazards associated with them. Figure 8 shows the locations of the five representative regions described below.

5.1. *Subduction Zones*

The Sunda megathrust is the dominant tectonic boundary of Indonesia in terms of length (5500 km; Fig. 9; Sieh, 2007). The Indo-Australian plate subducts beneath the Eurasian plate at a rate of $\sim$ 68 mm/year near Java (DeMets et al., 2010), building a volcanic island arc that forms much of Indonesia's land-mass, including the islands of Sumatra and Java (Fig. 8). Like many subduction systems worldwide, the Sunda megathrust has generated numerous tsunamigenic earthquakes: in the past 120 years, 12 earthquakes along this boundary caused wave heights greater than 1 m. Six of these caused great loss of life (Fig. 10; Table 2). Many of these events were shallow, slow rupture "tsunami earthquakes" (Kanamori, 1972), which have high

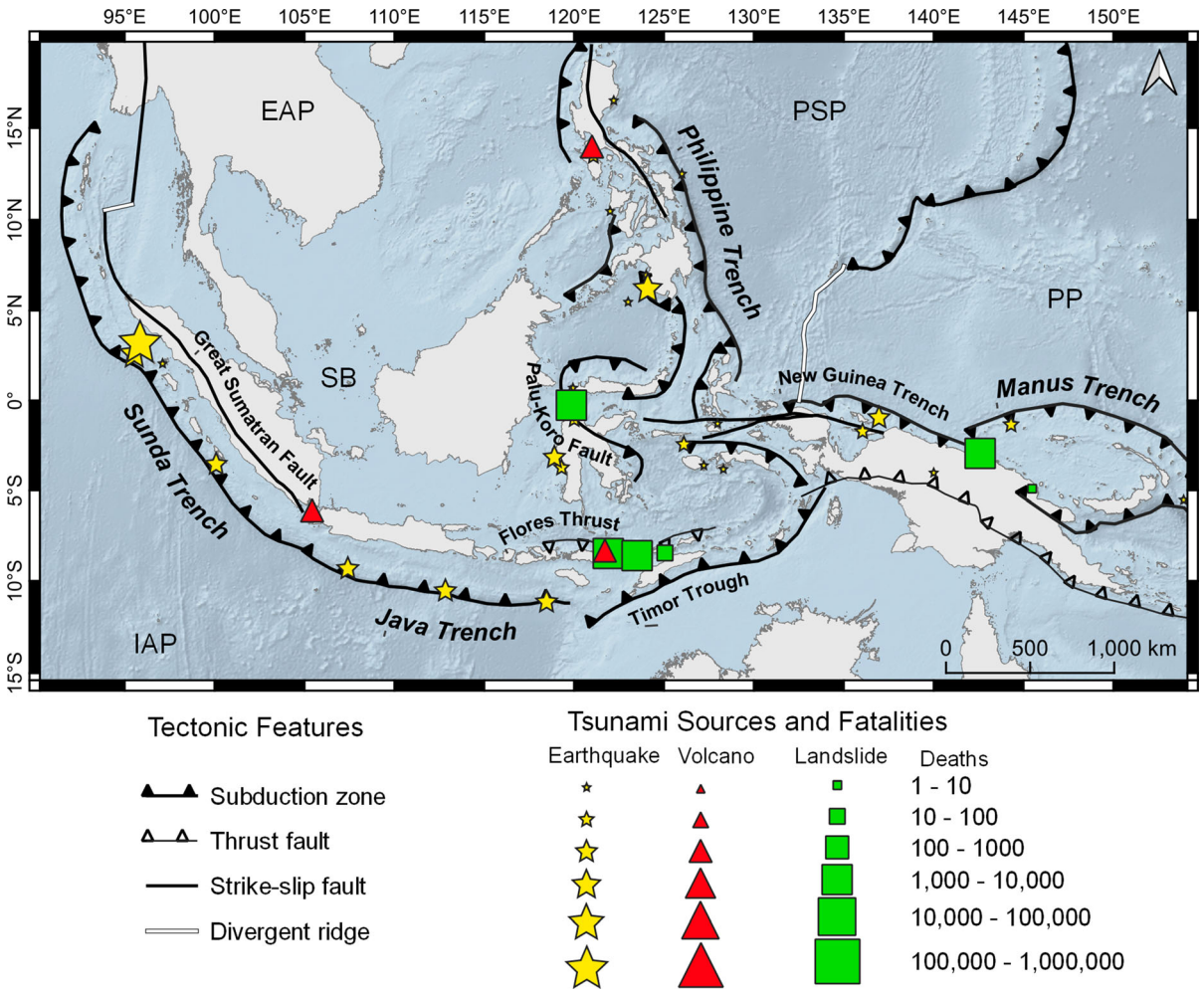

Figure 7

Map of tsunamis by source and number of fatalities in Indonesia and surrounding regions (1900–2020). Seven tsunamis generated by earthquakes, landslides, or both have caused over 1000 deaths each in the past 120 years. Two volcanically triggered tsunamis have also caused over 350 fatalities each in this region. Tsunami data are from NCEI/WDS (2021). Tectonic boundaries are modified from Bird (2003), Cipta et al. (2016), DeMets et al. (2010), Hall (2012) and Hutchings and Mooney (2021)

displacement and comparatively little ground shaking. In these cases, fault displacement is greater than 5 m and occurs at shallow subduction zone depths, which maximizes the displacement of the overlying water column and causes a large tsunami wave (Kanamori, 1972; Satake & Tanioka, 1999).

However, fault displacement alone cannot account for extreme water heights observed for some of the Sunda megathrust tsunamis. For example, a tsunami in 2006 (Fig. 10) generated locally concentrated water heights of 10–21 m at Nusa Kambangan on the south coast of Java (Fritz et al., 2007; Lavigne et al., 2007; Mori et al., 2007). The great water heights and geographic localization are inconsistent with a tsunami caused by fault displacement and inferred to signify a local landslide contribution (Fritz et al., 2007; Lavigne et al., 2007; Mori et al., 2007). This inference of a probable landslide contribution near Nusa Kambangan to the 2006 Java tsunami is in keeping with the increased recognition since 1998 of the tsunamigenic role of coseismic landslides (Løvholt et al., 2015). Hébert et al. (2012) present a combined earthquake-landslide source that closely

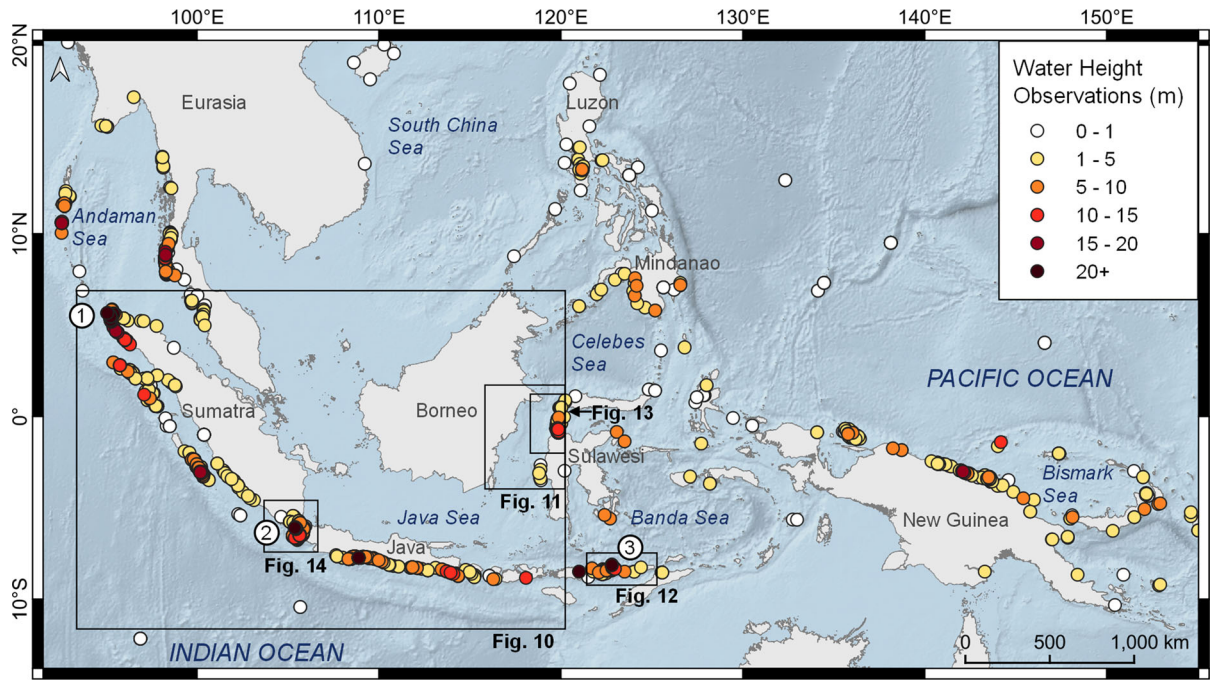

Figure 8
Map of maximum water height (MWH) for the Indonesian region, 1900–2020. The three tsunamis with highest MWH in this region are: (1) the 2004 Indian Ocean tsunami with a maximum runup of 50.9 m, (2) 2018 Anak Krakatau tsunami with a maximum runup of 85 m, and (3) 1992 Flores tsunami with a maximum runup of 26.2 m. Besides these three events, many other extreme MWHs greater than 5–10 m have been recorded in this region. Blue boxes indicate the locations of Figs. 10, 11, 12, 13, 14. Tsunami data are from NCEI/WDS (2021)

matches the water height observations recorded from the 2006 Java tsunami.

Evidence of past submarine landslides is incomplete and requires expensive marine surveys. The available evidence indicates that the number of submarine landslides along the Sunda megathrust increases to the southeast (Brune et al., 2010). It has been proposed that increased submarine landslides in this part of the forearc is linked to the regional characteristics of convergence (Brune et al., 2010). Convergence is perpendicular to the trench in the eastern portion of the Sunda megathrust (south of Central and East Java). Here, the forearc slope is steep (4.0°), and the subduction regime has been characterized as erosive (Kopp et al., 2006). Although evidence is still limited, preliminary studies suggest that erosive forearcs could be more susceptible to submarine landslides than accretionary forearcs (Kawamura et al., 2014). In contrast, at the NW Sunda trench (southwest of Sumatra, Fig. 10), convergence is oblique, and accretion of crustal material is extensive, resulting in a shallow 1.4° forearc slope (Clift & Vannuchi, 2004). The Sunda megathrust and other subduction interfaces in Indonesia, Papua New Guinea, and the Philippines present valuable opportunities to explore this hypothesis. If a correlation exists, specific hazard mitigation strategies could be better tailored to different areas along subduction zones according to the risk of tsunamigenic landslides.

5.2. *Continental Shelf*

The bathymetry of the Indonesian region varies greatly, ranging from deep trenches at subduction zones to shallow seas. The interior of the Sunda shelf represents the latter, as it lies mostly within the Sunda block (Fig. 7) and contains several land masses including the southeastern Eurasian continent, western Sulawesi, Borneo, Sumatra and Java (Fig. 8). The Sunda shelf is characterized by shallow bathymetry that was mostly above sea level during the last glacial

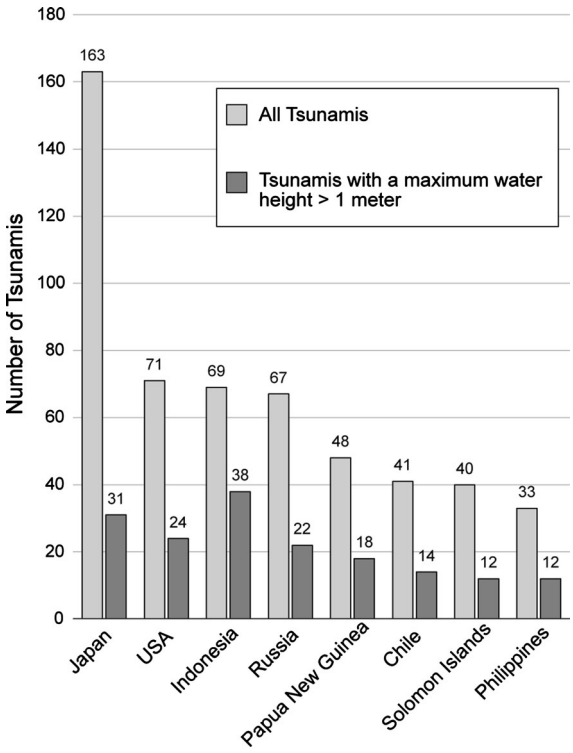

Figure 9
Top eight countries with the highest occurrence of tsunami sources from 1900 to 2020. The most tsunamis have been recorded in Japan. However, considering only tsunamis > 1 m, the greatest number occurred in Indonesia. Papua New Guinea, Indonesia and the Philippines are in the top eight countries. Data are from NCEI/WDS (2021)

maximum (Hanebuth et al., 2000). Sediment-laden passive continental margins have been known to yield large, low angle landslides and debris flows, some of which have been tsunamigenic (Masson et al., 2010). A prominent example of this environment is the Makassar Strait (Fig. 11) situated between Borneo and the Sunda shelf to the west and Sulawesi to the east. The Mahakam delta deposits sediment into the western margin of the strait, while the eastern (Sulawesi) margin is characterized by a seismogenic fold-thrust belt (Prasetya et al., 2001). The Makassar Strait throughflow, a strong thermohaline current, flows from north to south. This current causes slope-parallel erosion and sedimentation along the Makassar Strait, oversteepening the deltaic deposits east of Borneo. This process of slope-parallel deposition is suspected to have caused at least 19 submarine paleo-landslide deposits discovered on the eastern side of the strait (Brackenridge et al., 2020). These landslides may have generated large tsunamis. The nearby Brunei slide (Gee et al., 2007) in northwest Borneo is an example of a catastrophic submarine landslide that occurred in an environment of active rapid sedimentation, not unlike the Mahakam delta. The Brunei slide likely generated a catastrophic tsunami in the near field (Okal et al., 2011).

The velocity of a submarine landslide is an important factor that affects tsunamigenic potential (Løvholt et al., 2015; Okal & Synolakis, 2004). In the

Table 2

High fatality earthquake tsunamis associated with the Sunda-Java trench

Date	M_w	Source description	Tsunami fatalities	References
January 4, 1907	7.8	Slow "tsunami earthquake"	2188	Martin et al., (2019)
August 19, 1977	8.3	Outer rise normal fault	189	Gusman et al., (2009) and Lynnes and Lay (1988)
June 2, 1994	7.8	Slow "tsunami earthquake"	238	Abercrombie et al., (2001) and Maramai and Tinti (1997)
December 26, 2004	9.1	Megathrust earthquake	227,899	Grilli et al. (2007), Lay et al., (2005), and Synolakis and Okal (2005)
July 17, 2006	7.7	Slow "tsunami earthquake" with suspected local landslide at Nusa Kambangan	802	Fritz et al., (2007), Hébert et al., (2012) and Mori et al., (2007)
October 25, 2010	7.8	Slow "tsunami earthquake"	431	Satake et al., (2013) and Yue et al., (2014)

Tsunami Fatalities are from NCEI/WDS (2021). Earthquake magnitudes and source descriptions are from references in the last column

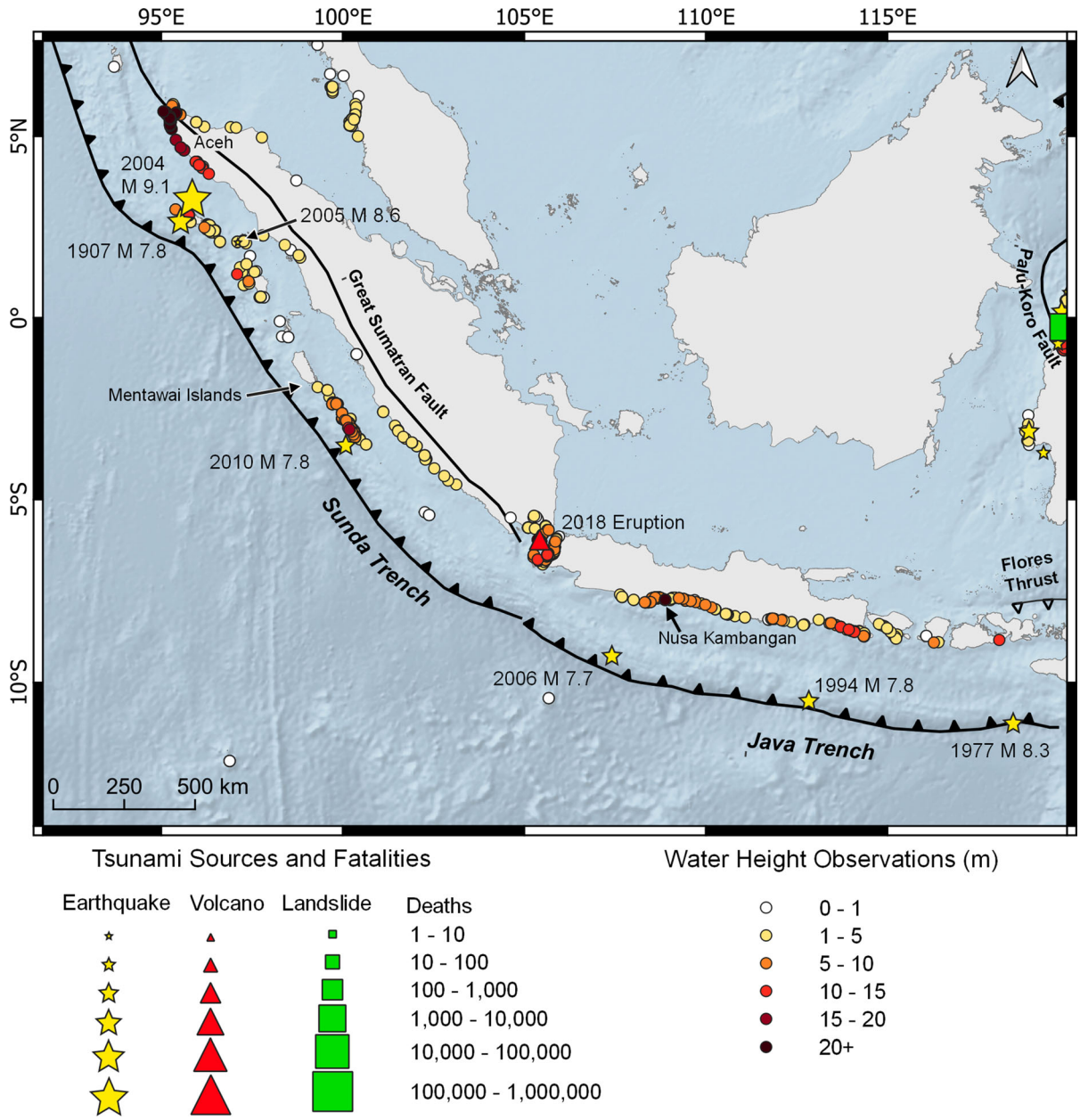

Figure 10

Tsunamis of the Sunda-Java trench that caused at least one recorded fatality (1900–2020). Tsunami source symbol is scaled according to the number of fatalities associated with the event. Runup observations are also shown as circles colored by runup height (m). Extreme runups here include Aceh, Sumatra (up to 50.9 m) from the December 2004 M 9.1 earthquake and tsunami, and Nusa Kambangan (up to 21 m) from the July 2006 M 7.7 earthquake and tsunami

southern Makassar Strait, deposits related to a submarine landslide (Fig. 11) were studied by Armandita et al. (2015). They concluded from the cohesive quality of the deposit, despite the weak sediments involved, that this landslide failed slowly and did not generate a tsunami. However, it is not known whether a region with a history of slow submarine ground failure is capable of producing

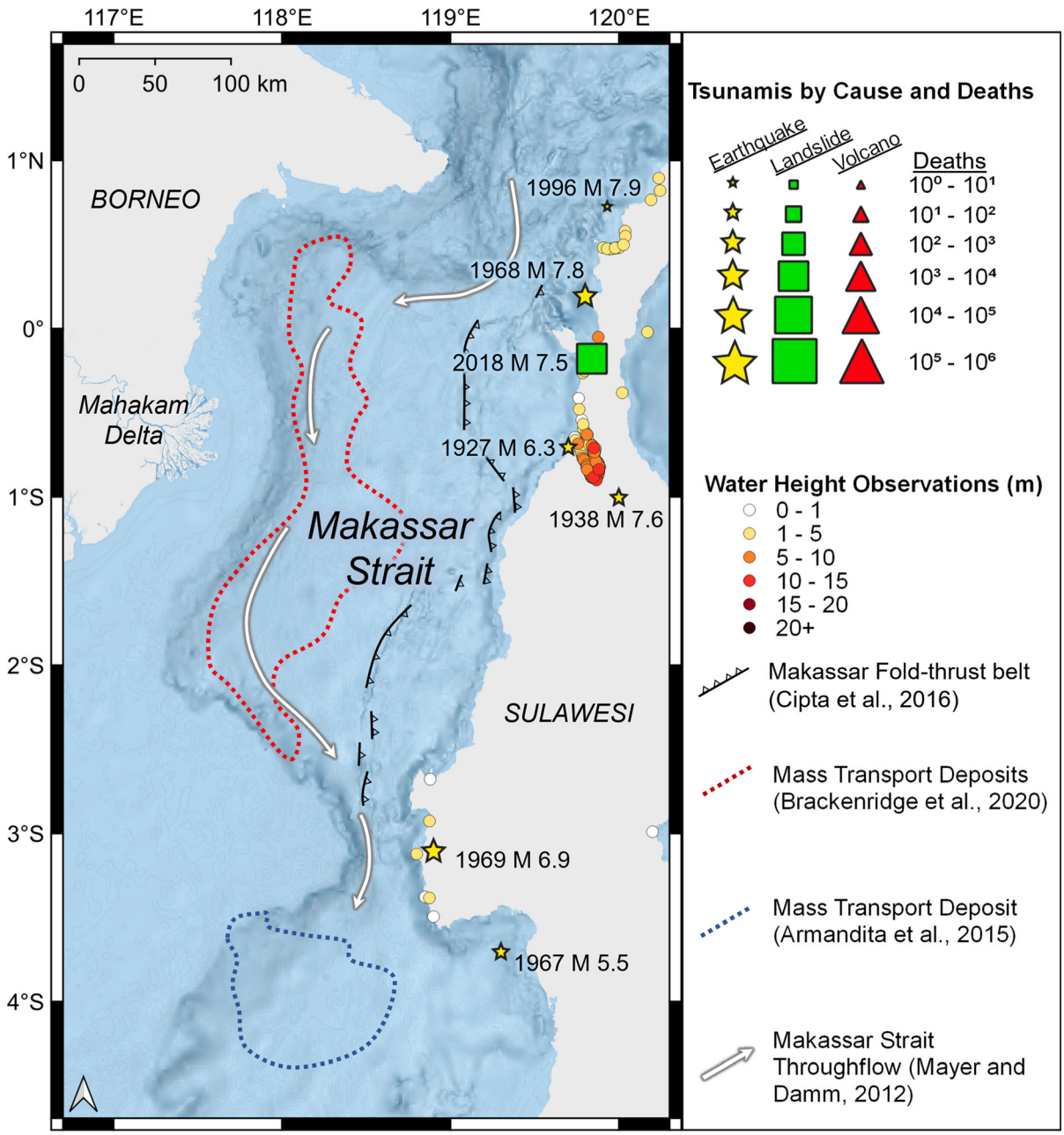

Figure 11
Landslide deposits in Makassar Strait. The red dotted line shows the location of 19 mass transport deposits identified by Brackenridge et al. (2020). The blue dotted line represents a mass transport deposit studied by Armandita et al. (2015). Note the sediment influx from the Mahakam Delta and over-steepened slopes on both sides of the strait, as well as tsunamigenic earthquakes on Sulawesi side. Earthquake symbols (stars) are scaled to the number of deaths recorded. Tsunami sources and water height observations are from NCEI/WDS (2021)

fast, tsunamigenic landslides. The steep slopes on both sides of the Makassar Strait, the regional history of landslides and seismicity, as well as the potential risk to coastal communities on either side of the strait, warrant further study of the probability of tsunamigenic landslides.

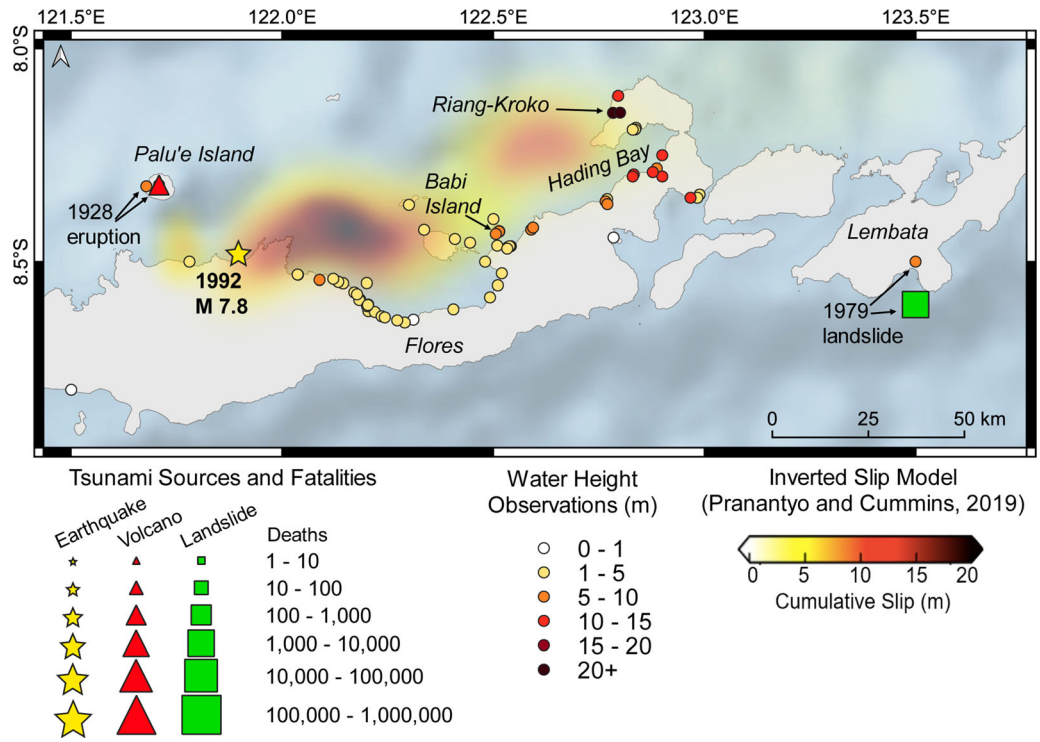

Figure 12

Tsunamis and water heights in the Flores Island region. Three tsunami events are shown: 1928, 1979, and 1992. All water height observations shown correspond to the 1992 earthquake and tsunami, except one observation for each of the 1928 and 1979 events, which are located immediately next to their respective source and labeled. Note that both the volcanic eruption of 1928 and the landslide of 1979 produced local, high (> 5 m) tsunamis. Babi Island is obscured by orange water height symbols. An inverted slip model of the 1992 fault rupture (Pranantyo & Cummins, 2019) is overlain. Note regions of high slip, closer to the earthquake epicenter, did not have the highest water heights, while in regions of lower slip such as Riang-Kroko and southern Hading Bay, extraordinary runups of 26.2 m and 14 m, respectively were observed

5.3. *Crustal Faults*

While subduction zone megathrust earthquakes are associated with most tsunamis in Indonesia (Fig. 8), crustal thrust and strike-slip earthquakes have also caused fatal, high-runup tsunamis in the recent past. Furthermore, the environments where these events occur can be conducive to amplification of propagating tsunami waves. Back-arc and strike-slip fault systems in this region accommodate strain by folding and incising oceanic and continental crust, which can lead to pronounced embayments and complicated landform geometries (Hall, 2012). These morphologies can be susceptible to landslides in addition to wave amplification. Additionally, arc volcanism in these regions provides steep slopes susceptible to failure, a tsunami triggering mechanism. Due to shorter faults and locally tsunamigenic mechanisms such as landslides and volcanos, a crustal fault tsunami may not have the long wavelength and impact radius of a large megathrust event. Nonetheless, as a result of the environmental factors outlined above, the local impact on coastal communities can be disproportionately severe.

5.3.1 *Thrust Faults*

In 1992, a M_w 7.8 earthquake associated with the Flores back arc thrust (Fig. 7) struck Flores Island (Fig. 12). The rupture area has been proposed to lie roughly along the north coast of Flores Island (Pranantyo & Cummins, 2019). A devastating tsunami resulted, and together with the earthquake killed at least 2080 people (NCEI/WDS, 2021). Roughly half of these fatalities are attributed to the tsunami (Yeh et al., 1993). According to the fault model by Pranantyo and Cummins (2019) (Fig. 12),

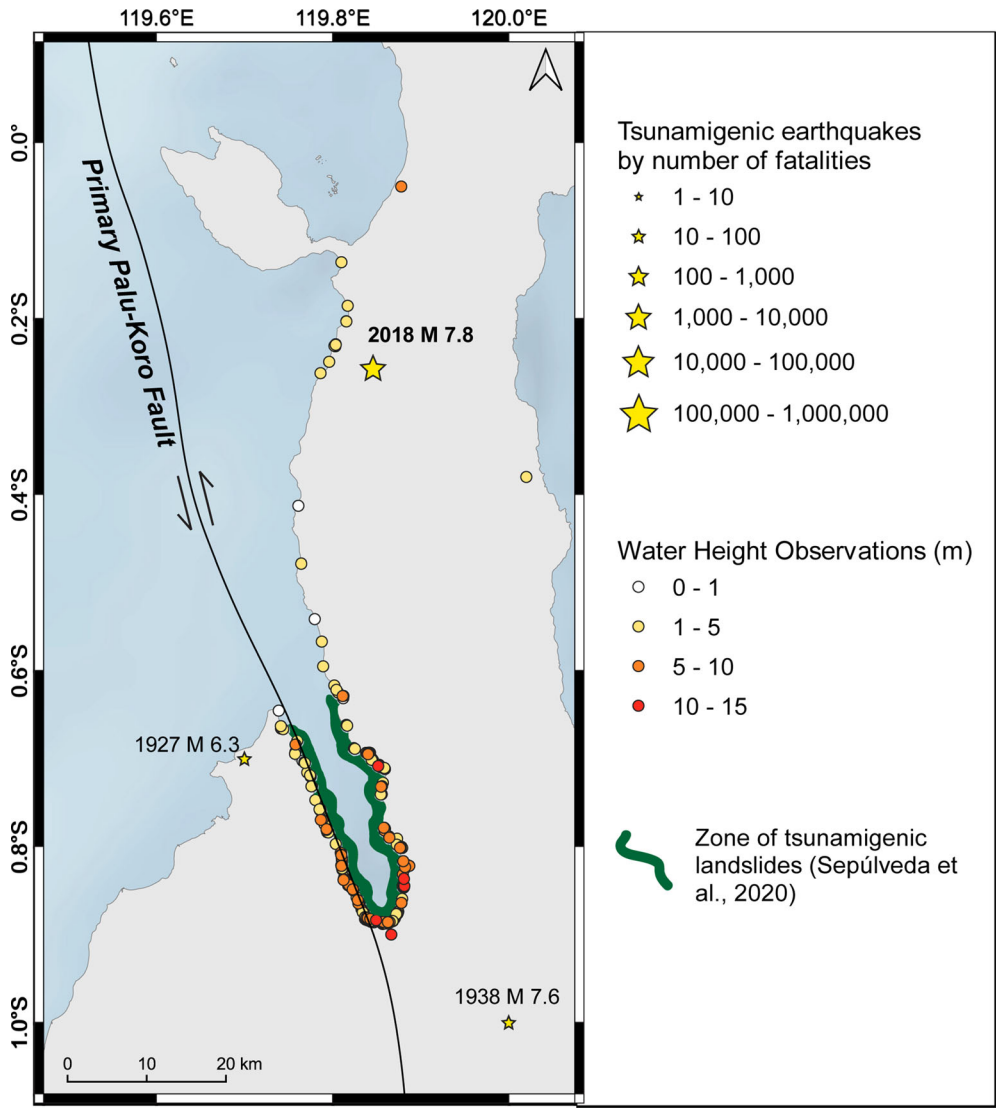

Figure 13
Palu Bay tsunamigenic earthquake epicenters, tsunami water heights and geometry. While the 1927 and 1938 tsunamigenic earthquakes are shown, water height observations displayed are from the Sept. 28, 2018 tsunami (earthquake epicenter shown by yellow star). The highest waves were observed at the head of Palu Bay. Green outline shows where coastal landslides were observed, some of which were tsunamigenic. The primary Palu-Koro fault is shown, but the region is dominated by secondary faults, several of which were active during the 2018 earthquake (Sepúlveda et al., 2020). Tsunami data are from NCEI/WDS (2021)

the tsunami was generated very close to shore (0–30 km in most places), with little opportunity for the waves to attenuate. Water height observations were unevenly distributed alongshore and extremely high (> 10 m) in some places (Fig. 12). Attempts to model the tsunami wave assuming that the source was solely due to the M_w 7.8 earthquake alone have fallen short of observed water heights, particularly in reproducing runups of 26.2 m in Riang-Kroko, as well as 10–14 m in Hading Bay (Hidayat et al., 1995; Imamura et al., 1995; Pranantyo & Cummins, 2019). The conclusion is that coastal landslides likely contributed to these extraordinary water heights (Hidayat et al., 1995; Pranantyo & Cummins, 2019; Tsuji et al., 1995; Yeh et al., 1993). This event illustrates how back-arc thrusts and other near-shore

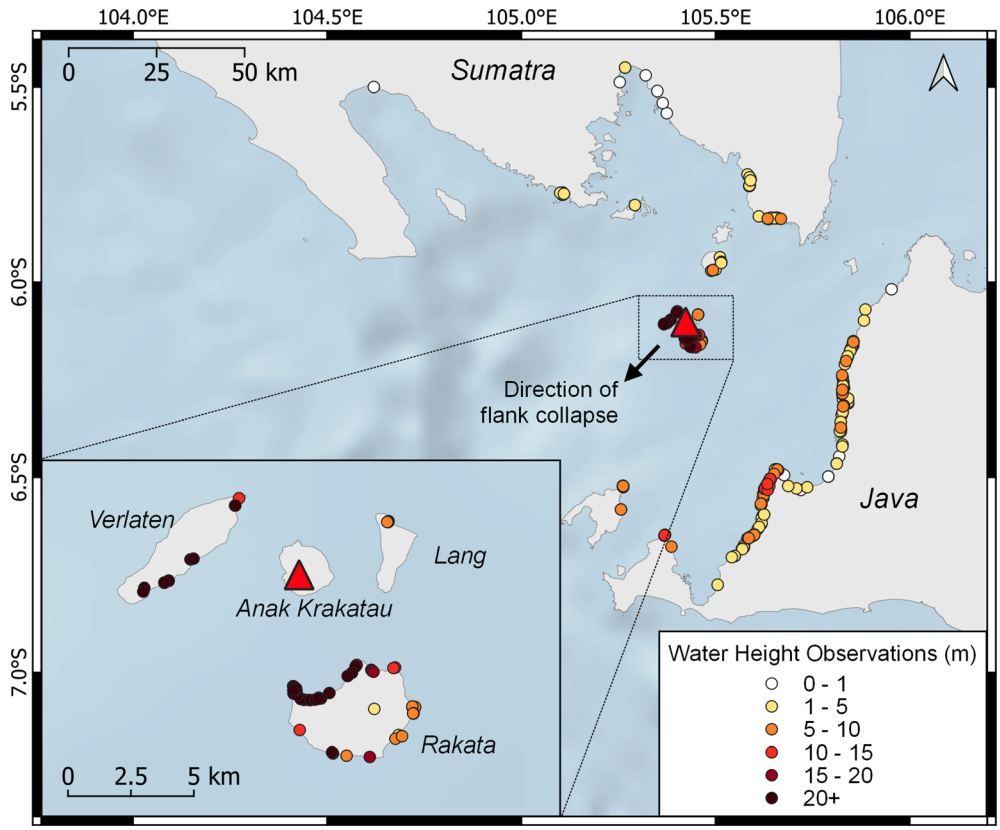

Figure 14
Anak Krakatau 2018 tsunami. Water heights shown are from the Dec. 22, 2018 tsunami caused by an eruption and failure of the southwestern flank (black arrow denotes direction of collapse). The three immediately adjacent islands, Verlaten, Lang, and Rakata, are remnants from the previous volcano island, Krakatau. The MWH from this tsunami was a runup of 85 m on Rakata. Note the SW-directed nature of greater water heights. Tsunami data are from NCEI/WDS (2021)

fault systems can both generate near-field tsunamis and trigger damaging tsunamigenic landslides.

The 1992 Flores event highlights the vulnerability of island communities to tsunamis. Because earthquake tsunamis are caused by seafloor deformation, the resulting waves involve the entire water column, unlike wind-driven waves. Thus, tsunami waves interact differently with bathymetric features such as shoals and islands (Yeh et al., 1994). Following the 1992 earthquake, water heights of 5.5–7.1 m were observed on the southern coast of Babi Island (Fig. 12; Tsuji et al., 1995), a part of the island that is normally protected from strong surface waves of the open ocean. These high water observations on the lee shore are attributed to positive interference from waves wrapping (refracting) around the circular island (Briggs et al., 1995; Kânoğlu & Synolakis, 1998; Yeh et al., 1994). Small islands like Babi Island are common in the Indonesian region, many of which reside near active fault zones that could trigger tsunamis. Coastal communities that are protected from wind-driven waves and normally have quiet waters may be unaware of and vulnerable to the refraction properties of a tsunami wave. The 1992 Flores tsunami highlights the particular need for analysis of potential tsunami hazard for small islands across this region, including those located in the back arc.

5.3.2 *Strike-Slip Faults*

A recent example of a devastating tsunami event with a complex source is the 2018 M_w 7.5 Sulawesi earthquake and landslide tsunami in Palu Bay,

Sulawesi (Omira et al., 2019) (Fig. 13). The primarily strike-slip earthquake associated with the Palu-Koro transform fault caused intense ground shaking, liquefaction, onshore landslides and coastal failure (Cilia & Mooney, 2021; Omira et al., 2019). Due to their minimal vertical seafloor displacement, strike-slip earthquakes are not commonly the source of such devastating tsunamis (Ward, 1980). However, largely enclosed bodies of water such as Palu Bay (Sulawesi, Indonesia) are susceptible to significant wave generation from strike-slip fault motion, particularly a supershear earthquake such as the 2018 event (Elbanna et al., 2021). What's more, strike-slip faults near coastlines are capable of creating precisely such elongate bays, for example Tomales Bay (California, USA). In the case of Palu, coastal failures (Omira et al., 2019; Sassa & Takagawa, 2019; Sepúlveda et al., 2020) and submarine landslides (Carvajal et al., 2019; Pakoksung et al., 2019) have both been proposed as potential sources for the tsunami waves. The models that best fit observed water heights incorporate contributions from three sources, including (1) coastal landslides, (2) submarine landslides, and (3) submarine fault motion (Cilia et al., 2021; Sassa & Takagawa, 2019; Sepúlveda et al., 2020).

5.3.3 Normal Faults

Normal fault earthquakes have also been known to cause tsunamis, though infrequently. In Indonesia, the 1977 Sumba tsunami (Gusman et al., 2009; Fig. 10; Table 2) was caused by a shallow M_w 8.3 normal-faulting earthquake in the subducting Indo-Australian plate just south of the Java trench (Lynnes & Lay, 1988). Outer rise earthquakes such as the 1977 Sumba earthquake occur under deeper waters than megathrust earthquakes. This increases the amplification effect of shoaling tsunami waves (Gusman et al., 2009), leading to high runups at shore.

5.4. Volcanic Sources

Arc volcanism in this region is widespread. Volcanos can rapidly produce material and deposit it at steep angles, causing unstable relief that is resolved by faulting and landslides (Moore et al., 1989). Volcanic activity can also be a seismic trigger for potentially tsunamigenic ground failure. A well-studied example in Indonesia is Anak Krakatau (Fig. 14). In December 2018, after 6 months of elevated volcanic activity, the southwestern flank of Anak Krakatau collapsed (Borrero et al., 2020; Grilli et al., 2019; Ye et al., 2020). The failed side of the volcano slid rapidly into the water, causing a tsunami that radiated to nearby shores and caused extreme water heights (up to 85 m) on the nearby Verlaten, Lang, and Rakata islands (Fig. 14). This event, which killed 437 people, was catastrophic but not surprising, because the volcano was known to be unstable and potentially tsunamigenic. In fact, a modeled collapse of the southwestern flank and resulting tsunami were produced six years prior (Giachetti et al., 2012), with results that were closely rendered by the actual 2018 event. Before the 2018 tsunami, this volcanic island had erupted several times in recorded history, causing tsunamis and countless fatalities. The 1883 eruption killed 36,417 people, mostly from tsunamis that struck nearby Java and Sumatra (NCEI/WDS, 2021; Paris et al., 2014). Another example of a tsunamigenic volcanic island in this region is Palu'e Island, which caused a tsunami in 1929 (Fig. 11). Volcanic islands are commonly densely populated, or close to populated coastlines, thus local tsunami risk to nearby communities is high.

6. Relative Sea Level Rise and Tsunami Hazard

Global sea level rose ~ 16 cm from 1902 to 2010 (Oppenheimer et al., 2019). Furthermore, global sea level rise is accelerating: from 2006 to 2015, the rate of global mean sea level rise was ~ 3.6 mm/year, compared to ~ 1.4 mm/year during 1901–1990 and ~ 2.1 mm/year during 1970–2015 (Oppenheimer et al., 2019). Increased hazards due to sea level rise are a global concern, particularly for coastal and island communities, including those in Indonesia, Papua New Guinea, and the Philippines (Nicholls & Cazenave, 2010). Small islands and low elevation coastal zones in these regions are also densely populated (Worldpop, 2018). A compounding issue is the significant tectonic and anthropogenic subsidence that is taking place in some densely

populated parts of Indonesia (Chaussard et al., 2013; Kuehn et al., 2009) and the Philippines (Rodolfo & Siringan, 2006), which increases the rate of local relative sea level rise.

Significant effects of sea level rise include increased flood risk (Vitousek et al., 2017) from storms and tsunami inundation, as well as permanent submersion of populated areas (Oppenheimer et al., 2019). The tropics in particular are projected to undergo increased frequency in extreme flooding events, due to as little as 5–10 cm of sea level rise (Vitousek et al., 2017). Sea level rise is a growing topic of interest for tsunami hazard projections in vulnerable regions, particularly on the timescale of community development planning (Meilianda et al., 2019). A new variation of probabilistic tsunami hazard assessment works to account for the influence of the rising sea level (Sepúlveda et al., 2021). In southern China, a projected 50 cm of sea level rise by 2060 is predicted to double the tsunami hazard (Li et al., 2018). Indonesia and surrounding regions face the challenges of low elevation coastal populations, high proportions of reclaimed land, and nearby tsunamigenic sources.

Rising sea level will not only affect tsunami inundation and population vulnerability; sea level rise will also have broader effects on geomorphologic and tectonic processes (Leatherman et al., 2000; Limber et al., 2018; McGuire, 2010). As sea level rise alters the coastal and shelf environment, local tsunami hazards may develop, including shallow bathymetry and irregular geometries that can cause wave amplification. Furthermore, sea level rise has implications for erosion of coastal cliffs (Limber et al., 2018) and offshore slope stability. Sea level rise may influence the frequency of submarine landslides by increasing failure preconditioning mechanisms such as storm wave loading and sedimentation patterns (Tappin, 2010). The role of climate-cycling sedimentation patterns in the occurrence of tsunamigenic paleolandslides is studied (Bondevik et al., 2019). However, concrete implications of climate change for future tsunami hazard remain a pertinent and largely unexplored research question.

7. Conclusions

An analysis of tsunami occurrence worldwide for the period 1900–2020 provides a broad overview of the distribution and maximum wave heights of tsunamis globally. We have documented the importance of landslide-sourced tsunamis, which pose an underestimated threat to many coastal communities. Our analysis leads to the following conclusions:

(1) Fatalities can generally result from tsunamis with maximum water heights > 1 m (Fig. 4). Indonesia has the greatest number of tsunamis > 1 m (Fig. 9), making tsunami hazard mitigation a high priority for this country.

(2) In many regions deadly tsunamis have multiple causes (Figs. 3 and 5); Indonesia, the Philippines, and Papua New Guinea have experienced devastating tsunamis not just from megathrust earthquakes, but also from intraplate crustal earthquakes, landslides and volcanic eruptions. These sources can also occur in combination, such as a landslide triggered by an earthquake or volcano eruption. In this region, four out of the seven deadliest (> 1000 deaths) tsunamis involved landslides. Three of these seven events were not in active subduction zones, where most tsunami research is dedicated (Fig. 7).

(3) Whereas earthquakes alone cause the vast majority of all recorded tsunamis, landslide-generated tsunamis are disproportionately represented among those events that cause deaths. Landslides cause 24% of all fatal tsunamis (Fig. 5b). However, hazards from landslide tsunamis are underestimated due to the logistical difficulty to document submarine and subaerial landslides. A major contributor to the high fatalities is the great water height achieved by landslide tsunamis. The median maximum water height from landslide tsunamis is ten times greater than that from earthquake tsunamis (Table 1). Every tsunami with a maximum water height over 56 m was due in part to a landslide (Fig. 4).

Acknowledgements

We thank reviewers Emile Okal, David Scholl, Dale Bird, Laura Sammon, Halle Putera, Johana Barrera-Gonzalez, Anna Baker, Marcella Cilia, Carol Barrera-Lopez, and Sean Hutchings, as well as two anonymous peer reviewers for their helpful comments. This work was supported by the US Geological Survey Earthquake Hazards Program and the US Agency for International Development, Bureau of Humanitarian Affairs.

Funding

This project was funded by the Bureau of Humanitarian Affairs within the US Agency for International Development and the US Geological Survey, Earthquake Science Center.

Availability of data and material

This work was made possible by the following online data sources: NOAA NCEI/WDS Global Historical Tsunami Database (www.ngdc.noaa.gov/hazard), Gebco (www.gebco.net), WorldPop (www.worldpop.org), Global Volcanism Program, Smithsonian Institution (https://volcano.si.edu/).

Software availability

Map figures were made using version 3.16 of the open-source Geographic Information Systems software QGIS (https://www.qgis.org/en/site/).

Declarations

Conflict of interest The authors have no relevant financial or non-financial interests to disclose.

References

Abercrombie, R. E., Antolik, M., Felzer, K., & Ekström, G. (2001). The 1994 Java tsunami earthquake: Slip over a subducting seamount. *Journal of Geophysical Research: Solid Earth, 106*(B4), 6595–6607. https://doi.org/10.1029/2000JB900403

Arcos, N. P., Dunbar, P. K., Stroker, K. J., & Kong, L. S. L. (2019). The impact of post-tsunami surveys on the NCEI/WDS global historical tsunami database. *Pure and Applied Geophysics, 176*(7), 2809–2829. https://doi.org/10.1007/s00024-019-02191-7

Armandita, C., Morley, C., & Rowell, P. (2015). Origin, structural geometry, and development of a giant coherent slide: The South Makassar Strait mass transport complex. *Geosphere, 11*(2), 376–403. https://doi.org/10.1130/GES01077.1

Bardet, J.-P., Synolakis, C. E., Davies, H. L., Imamura, F., & Okal, E. A. (2003). Landslide tsunamis: Recent findings and research directions. *Pure and Applied Geophysics, 160*(10), 1793–1809. https://doi.org/10.1007/s00024-003-2406-0

Bird, P. (2003). An updated digital model of plate boundaries. *Geochemistry, Geophysics, Geosystems*. https://doi.org/10.1029/2001GC000252

Bondevik, S. (2019). Tsunami from the Storegga landslide. *Encyclopedia of Complexity and Systems Science*. https://doi.org/10.1007/978-3-642-27737-5_644-1

Borrero, J. C., Solihuddin, T., Fritz, H. M., Lynett, P. J., Prasetya, G. S., Skanavis, V., Husrin, S., Kushendratno, Kongko, W., Istiyanto, D. C., Daulat, A., Purbani, D., Salim, H. L., Hidayat, R., Asvaliantina, V., Usman, M., Kodijat, A., Son, S., & Synolakis, C. E. (2020). Field survey and numerical modelling of the December 22, 2018 Anak Krakatau tsunami. *Pure and Applied Geophysics, 177*(6), 2457–2475. https://doi.org/10.1007/s00024-020-02515-y

Brackenridge, R. E., Nicholson, U., Sapiie, B., Stow, D., & Tappin, D. R. (2020). Indonesian Throughflow as a preconditioning mechanism for submarine landslides in the Makassar Strait. *Geological Society, London, Special Publications, 500*(1), 195–217. https://doi.org/10.1144/SP500-2019-171

Briggs, M. J., Synolakis, C. E., Harkins, G. S., & Green, D. R. (1995). Laboratory experiments of tsunami runup on a circular island. *Pure and Applied Geophysics, 144*, 569–593. https://doi.org/10.1007/BF00874384

Brune, S., Babeyko, A. Y., Ladage, S., & Sobolev, S. V. (2010). Landslide tsunami hazard in the Indonesian Sunda Arc. *Natural Hazards and Earth System Sciences, 10*(3), 589–604. https://doi.org/10.5194/nhess-10-589-2010

Carvajal, M., Araya-Cornejo, C., Sepúlveda, I., Melnick, D., & Haase, J. S. (2019). Nearly instantaneous tsunamis following the Mw 7.5 2018 Palu earthquake. *Geophysical Research Letters, 46*(10), 5117–5126. https://doi.org/10.1029/2019GL082578

Chaussard, E., Amelung, F., Abidin, H., & Hong, S.-H. (2013). Sinking cities in Indonesia: ALOS PALSAR detects rapid subsidence due to groundwater and gas extraction. *Remote Sensing of Environment, 128*, 150–161. https://doi.org/10.1016/j.rse.2012.10.015

Cilia, M. G., Mooney, W. D., & Nugroho, C. (2021). Field insights and analysis of the 2018 Mw 7.5 Palu, Indonesia earthquake, tsunami and landslides. *Pure and Applied Geophysics, 178*, 4891–4920. https://doi.org/10.1007/s00024-021-02852-6

Cipta, A., Robiana, R., Griffin, J., Horspool, N., Hidayati, S., & Cummins, P. (2016). A probabilistic seismic hazard assessment for Sulawesi, Indonesia. *Geological Society, London, Special Publications*. https://doi.org/10.1144/SP441.6

Clift, P., & Vannucchi, P. (2004). Controls on tectonic accretion versus erosion in subduction zones: Implications for the origin and recycling of the continental crust. *Reviews of Geophysics*. https://doi.org/10.1029/2003RG000127

DeMets, C., Gordon, R. G., & Argus, D. F. (2010). Geologically current plate motions. *Geophysical Journal International, 181*(1), 1–80. https://doi.org/10.1111/j.1365-246X.2009.04491.x

Elbanna, A., Abdelmeguid, M., Ma, X., Amlani, F., Bhat, H. S., Synolakis, C., & Rosakis, A. J. (2021). Anatomy of strike-slip fault tsunami genesis. *Proceedings of the National Academy of Sciences, 118*(19), e2025632118. https://doi.org/10.1073/pnas.2025632118

Fritz, H. M., Kongko, W., Moore, A., McAdoo, B., Goff, J., Harbitz, C., & Synolakis, C. (2007). Extreme runup from the 17 July 2006 Java tsunami. *Geophysical Research Letters*. https://doi.org/10.1029/2007GL029404

Gee, M., Uy, H. S., Warren, J., Morley, C., & Lambiase, J. J. (2007). The Brunei slide: A giant submarine landslide on the North West Borneo Margin revealed by 3D seismic data. *Marine Geology, 246*, 9–23. https://doi.org/10.1016/j.margeo.2007.07.009

Giachetti, T., Paris, R., Kelfoun, K., & Ontowirjo, B. (2012). Tsunami hazard related to a flank collapse of Anak Krakatau Volcano, Sunda Strait, Indonesia. *Geological Society, London, Special Publications, 361*(1), 79–90. https://doi.org/10.1144/SP361.7

Global Volcanism Program. (2013). Volcanoes of the World, v. 4.9.2. Venzke, E (ed.). Smithsonian Institution. https://doi.org/10.5479/si.GVP.VOTW4-2013

Grilli, S. T., Harris, J., Tajali-Bakhsh, T. S., Tappin, D., Masterlark, T., Kirby, J., Shi, F., & Ma, G. (2012). Recent progress in the nonlinear and dispersive modeling of tsunami generation and coastal impact: Application to Tohoku 2011. *Proc. 13th Journées Hydrodynamiques* (Chatou, France, Nov. 21–23, 2012), 16 pp.

Grilli, S. T., Ioualalen, M., Asavanant, J., Shi, F., Kirby, J. T., & Watts, P. (2007). Source constraints and Model simulation of the December 26, 2004, Indian Ocean tsunami. *Journal of Waterway, Port, Coastal, and Ocean Engineering*, *133*(6), 414–428. https://doi.org/10.1061/(ASCE)0733-950X(2007)133:6(414)

Grilli, S. T., Tappin, D. R., Carey, S., Watt, S. F. L., Ward, S. N., Grilli, A. R., Engwell, S. L., Zhang, C., Kirby, J. T., Schambach, L., & Muin, M. (2019). Modelling of the tsunami from the December 22, 2018 lateral collapse of Anak Krakatau volcano in the Sunda Straits, Indonesia. *Scientific Reports, 9*(1), 11946. https://doi.org/10.1038/s41598-019-48327-6

Gusiakov, V. K. (2009). Tsunami history: Recorded. *The Sea, 15*, 23–53.

Gusiakov, V. K. (2020). Global occurrence of large tsunamis and tsunami-like waves within the last 120 years (1900–2019). *Pure and Applied Geophysics, 177*(3), 1261–1266. https://doi.org/10.1007/s00024-020-02437-9

Gusman, A., Tanioka, Y., Matsumoto, H., & Iwasaki, S.-I. (2009). analysis of the tsunami generated by the great 1977 sumba earthquake that occurred in Indonesia. *Bulletin of the Seismological Society of America, 99*, 2169–2179. https://doi.org/10.1785/0120080324

Hall, R. (2012). Late Jurassic-Cenozoic reconstructions of the Indonesian region and the Indian Ocean. *Tectonophysics, 570–571*, 1–41. https://doi.org/10.1016/j.tecto.2012.04.021

Hamilton, W. B. (1979). Tectonics of the Indonesian region. USGS Professional Paper 1078, 345 pp., 1 map. https://doi.org/10.3133/pp1078

Hanebuth, T., Stattegger, K., & Grootes, P. M. (2000). Rapid flooding of the Sunda Shelf: A late-glacial sea-level record. *Science, 288*(5468), 1033–1035. https://doi.org/10.1126/science.288.5468.1033

Harbitz, C. B., Løvholt, F., & Bungum, H. (2014). Submarine landslide tsunamis: How extreme and how likely? *Natural Hazards, 72*(3), 1341–1374. https://doi.org/10.1007/s11069-013-0681-3

Hébert, H., Burg, P.-E., Binet, R., Lavigne, F., Allgeyer, S., & Schindelé, F. (2012). The 2006 July 17 Java (Indonesia) tsunami from satellite imagery and numerical modelling: A single or complex source? *Geophysical Journal International, 191*(3), 1255–1271. https://doi.org/10.1111/j.1365-246X.2012.05666.x

Hidayat, D., Barker, J. S., & Satake, K. (1995). Modeling the seismic source and tsunami generation of the December 12, 1992 Flores Island, Indonesia, earthquake. *Pure and Applied Geophysics, 144*(3), 537–554. https://doi.org/10.1007/BF00874382

Hutchings, S. J., & Mooney, W. D. (2021). The Seismicity of Indonesia and tectonic implications. *Geochemistry, Geophysics and Geosystems, 22*, e2021GC009812. https://doi.org/10.1029/2021GC009812

Imamura, F., Gica, E., Takahashi, T., & Shuto, N. (1995). Numerical simulation of the 1992 Flores tsunami: Interpretation of tsunami phenomena in northeastern Flores Island and damage at Babi Island. *Pure and Applied Geophysics, 144*(3), 555–568. https://doi.org/10.1007/BF00874383

Kanamori, H. (1972). Mechanism of tsunami earthquakes. *Physics of the Earth and Planetary Interiors, 6*(5), 346–359. https://doi.org/10.1016/0031-9201(72)90058-1

Kânoğlu, U., & Synolakis, C. E. (1998). Long wave runup on piecewise linear topographies. *Journal of Fluid Mechanics, 374*, 1–28. https://doi.org/10.1017/S0022112098002468

Kânoğlu, U., Tanioka, Y., Okal, E. A., Baptista, M. A., & Rabinovich, A. B. (2020). Introduction to "Twenty-five years of modern tsunami science following the 1992 Nicaragua and Flores Island tsunamis, volume II." *Pure and Applied Geophysics, 177*(3), 1183–1191. https://doi.org/10.1007/s00024-020-02451-x

Kawamura, K., Laberg, J. S., & Kanamatsu, T. (2014). Potential tsunamigenic submarine landslides in active margins. *Marine Geology, 356*, 44–49. https://doi.org/10.1016/j.margeo.2014.03.007

Kopp, H., Flueh, E., Petersen, C., Weinrebe, W., Wittwer, A., & Scientists, M. (2006). The Java margin revisited: Evidence for subduction erosion off Java. *Earth and Planetary Science Letters, 242*(1–2), 130–142. https://doi.org/10.1016/j.epsl.2005.11.036

Kuehn, F., Albiol, D., Cooksley, G., Duro, J., Granda, J., Haas, S., Hoffmann-Rothe, A., & Murdohardono, D. (2009). Detection of land subsidence in Semarang, Indonesia, using stable points network (SPN) technique. *Environmental Earth Sciences, 60*, 909–921. https://doi.org/10.1007/s12665-009-0227-x

Lavigne, F., Gomez, C., Giffo, M., Wassmer, P., Hoebreck, C., Mardiatno, D., Prioyono, J., & Paris, R. (2007). Field observations of the 17 July 2006 Tsunami in Java. *Natural Hazards and Earth System Sciences, 7*(1), 177–183. https://doi.org/10.5194/nhess-7-177-2007

Lay, T., Kanamori, H., Ammon, C. J., Nettles, M., Ward, S. N., Aster, R. C., Beck, S. L., Bilek, S. L., Brudzinski, M. R., Butler, R., & DeShon, H. R. (2005). The Great Sumatra-Andaman Earthquake of 26 December 2004. *Science (new York, N.y.), 308*, 1127–1133. https://doi.org/10.1126/science.1112250

Leatherman, S. P., Zhang, K., & Douglas, B. C. (2000). Sea level rise shown to drive coastal erosion. *Eos, Transactions American Geophysical Union, 81*, 55–57. https://doi.org/10.1029/00EO00034

Li, L., Switzer, A., Wang, Y., Chan, C.-H., Qiu, Q., & Weiss, R. (2018). A modest 0.5-m rise in sea level will double the tsunami hazard in Macau. *Science Advances, 4*, eaat1180. https://doi.org/10.1126/sciadv.aat1180

Limber, P. W., Barnard, P. L., Vitousek, S., & Erikson, L. H. (2018). A model ensemble for projecting multidecadal coastal cliff retreat during the 21st century. *Journal of Geophysical Research: Earth Surface, 123*(7), 1566–1589. https://doi.org/10.1029/2017JF004401

Løvholt, F., Pedersen, G., Harbitz, C. B., Glimsdal, S., & Kim, J. (2015). On the characteristics of landslide tsunamis. *Philosophical Transactions of the Royal Society a: Mathematical, Physical and Engineering Sciences, 373*(2053), 20140376. https://doi.org/10.1098/rsta.2014.0376

Lynnes, C., & Lay, T. (1988). Source process of the great 1977 Sumba earthquake. *Journal of Geophysical Research, 931*, 13407–13420. https://doi.org/10.1029/JB093iB11p13407

Maramai, A., & Tinti, S. (1997). The 3 June 1994 Java tsunami: A post-event survey of the coastal effects. *Natural Hazards, 15*(1), 31–49. https://doi.org/10.1023/A:1007957224367

Martin, S., Li, L., Okal, E., Morin, J., Tetteroo, A., Switzer, A., & Sieh, K. (2019). Reassessment of the 1907 Sumatra "tsunami earthquake" based on macroseismic, seismological, and tsunami observations, and modeling. *Pure and Applied Geophysics, 176*, 2831–2868. https://doi.org/10.1007/s00024-019-02134-2

Masson, D. G., Wynn, R. B., & Talling, P. J. (2010). Large landslides on passive continental margins: Processes, hypotheses and outstanding questions. In D. C. Mosher, R. C. Shipp, L. Moscardelli, J. D. Chaytor, C. D. P. Baxter, H. J. Lee, & R. Urgeles (Eds.), *Submarine mass movements and their consequences* (pp. 153–165). Springer Netherlands. https://doi.org/10.1007/978-90-481-3071-9_13

McGuire, B. (2010). Potential for a hazardous geospheric response to projected future climate changes. *Philosophical Transactions: Mathematical, Physical and Engineering Sciences, 368*(1919), 2317–2345.

Meilianda, E., Pradhan, B., Syamsidik, Comfort, L. K., Alfian, D., Juanda, R., Syahreza, S., & Munadi, K. (2019). Assessment of post-tsunami disaster land use/land cover change and potential impact of future sea-level rise to low-lying coastal areas: A case study of Banda Aceh coast of Indonesia. *International Journal of Disaster Risk Reduction, 41*, 101292. https://doi.org/10.1016/j.ijdrr.2019.101292

Moore, J. G., Clague, D. A., Holcomb, R. T., Lipman, P. W., Normark, W. R., & Torresan, M. E. (1989). Prodigious submarine landslides on the Hawaiian Ridge. *Journal of Geophysical Research: Solid Earth, 94*(B12), 17465–17484. https://doi.org/10.1029/JB094iB12p17465

Mori, J., Mooney, W. D., Afnimar, Kurniawan, S., Anaya, A. I., & Widiyantoro, S. (2007). The 17 July 2006 tsunami earthquake in West Java, Indonesia. *Seismological Research Letters, 78*(2), 201–207. https://doi.org/10.1785/gssrl.78.2.201

National Geophysical Data Center / World Data Service: NCEI/WDS Global historical tsunami database. NOAA National Centers for Environmental Information, https://doi.org/10.7289/V5PN93H7. Accessed Dec 2021.

Nicholls, R., & Cazenave, A. (2010). Sea-level rise and its impact on coastal zones. *Science, 328*, 1517–1520. https://doi.org/10.1126/science.1185782

Okal, E. A. (2019). Twenty-five years of progress in the science of "geological" tsunamis following the 1992 Nicaragua and Flores events. *Pure and Applied Geophysics, 176*(7), 2771–2793. https://doi.org/10.1007/s00024-019-02244-x

Okal, E. A., & Synolakis, C. E. (2004). Source discriminants for near-field tsunamis. *Geophysical Journal International, 158*(3), 899–912. https://doi.org/10.1111/j.1365-246X.2004.02347.x

Okal, E. A., Synolakis, C. E., & Kalligeris, N. (2011). Tsunami Simulations for Regional Sources in the South China and Adjoining Seas. *Pure and Applied Geophysics, 168*(6–7), 1153–1173. https://doi.org/10.1007/s00024-010-0230-x

Omira, R., Dogan, G. G., Hidayat, R., Husrin, S., Prasetya, G., Annunziato, A., Proietti, C., Probst, P., Paparo, M. A., Wronna, M., Zaytsev, A., Pronin, P., Giniyatullin, A., Putra, P. S., Hartanto, D., Ginanjar, G., Kongko, W., Pelinovsky, E., & Yalciner, A. C. (2019). The September 28th, 2018, tsunami in Palu-Sulawesi, Indonesia: A post-event field survey. *Pure and Applied Geophysics, 176*(4), 1379–1395. https://doi.org/10.1007/s00024-019-02145-z

Oppenheimer, M., Glavovic, B.C., Hinkel, J., van de Wal, R., Magnan, A.K., Abd-Elgawad, A., Cai, R., Cifuentes-Jara, M., DeConto, R.M., Ghosh, T., Hay, J., Isla, F., Marzeion, B., Meyssignac, B., Sebesvari, Z. (2019). Sea level rise and implications for low-lying islands, coasts and communities. In H.-O. Pörtner, D.C. Roberts, V. Masson-Delmotte, P. Zhai, M. Tignor, E. Poloczanska, K. Mintenbeck, A. Alegría, M. Nicolai, A. Okem, J. Petzold, B. Rama, N.M. Weyer (Eds.), IPCC Special Report on the Ocean and Cryosphere in a Changing Climate.

Pakoksung, K., Suppasri, A., Imamura, F., Athanasius, C., Omang, A., & Muhari, A. (2019). Simulation of the submarine landslide tsunami on 28 September 2018 in Palu Bay, Sulawesi Island, Indonesia, Using a Two-Layer Model. *Pure and Applied Geophysics, 176*(8), 3323–3350. https://doi.org/10.1007/s00024-019-02235-y

Paris, R., Wassmer, P., Lavigne, F., Belousov, A., Belousova, M., Iskandarsyah, Y., Benbakkar, M., Ontowirjo, B., & Mazzoni, N. (2014). Coupling eruption and tsunami records: The Krakatau

1883 case study, Indonesia. *Bulletin of Volcanology, 76*, 814. https://doi.org/10.1007/s00445-014-0814-x

Pranantyo, I. R., & Cummins, P. R. (2019). Multi-data-type source estimation for the 1992 Flores earthquake and tsunami. *Pure and Applied Geophysics, 176*(7), 2969–2983. https://doi.org/10.1007/s00024-018-2078-4

Prasetya, G., de Lange, W., & Healy, T. (2001). The Makassar Strait tsunamigenic region, Indonesia. *Natural Hazards, 24*, 295–307. https://doi.org/10.1023/A:1012297413280

QGIS. (2021). QGIS Geographic Information System. QGIS Association. http://www.qgis.org

Rabinovich, A. (2020). Twenty-seven years of progress in the science of meteorological tsunamis following the 1992 Daytona Beach event. *Pure and Applied Geophysics*. https://doi.org/10.1007/s00024-019-02349-3

Rodolfo, K. S., & Siringan, F. P. (2006). Global sea-level rise is recognised, but flooding from anthropogenic land subsidence is ignored around northern Manila Bay, Philippines. *Disasters, 30*(1), 118–139. https://doi.org/10.1111/j.1467-9523.2006.00310.x

Sassa, S., & Takagawa, T. (2019). Liquefied gravity flow-induced tsunami: First evidence and comparison from the 2018 Indonesia Sulawesi earthquake and tsunami disasters. *Landslides, 16*(1), 195–200. https://doi.org/10.1007/s10346-018-1114-x

Satake, K., Nishimura, Y., Putra, P. S., Gusman, A. R., Sunendar, H., Fujii, Y., Tanioka, Y., Latief, H., & Yulianto, E. (2013). Tsunami source of the 2010 Mentawai, Indonesia earthquake inferred from tsunami field survey and waveform modeling. *Pure and Applied Geophysics, 170*(9), 1567–1582. https://doi.org/10.1007/s00024-012-0536-y

Satake, K., & Tanioka, Y. (1999). Sources of tsunami and tsunamigenic earthquakes in subduction zones. *Pure and Applied Geophysics, 154*, 17. https://doi.org/10.1007/s000240050240

Sepúlveda, I., Haase, J. S., Carvajal, M., Xu, X., & Liu, P. L. F. (2020). Modeling the sources of the 2018 Palu, Indonesia, tsunami using videos from social media. *Journal of Geophysical Research: Solid Earth*. https://doi.org/10.1029/2019JB018675

Sepúlveda, I., Haase, J. S., Liu, P.L.-F., Grigoriu, M., & Winckler, P. (2021). Non-stationary probabilistic tsunami hazard assessments incorporating climate-change-driven sea level rise. *Earth's Future, 9*(6), e2021EF002007. https://doi.org/10.1029/2021EF002007

Sieh, K. (2007). The Sunda megathrust—past, present and future. *Journal of Earthquake and Tsunami, 1*(01), 1–19. https://doi.org/10.1142/S179343110700002X

Synolakis, C., & Okal, E. (2005). 1992–2002: Perspective on a decade of post-tsunami surveys. In *Adv. Nat. Technol. Hazards* (vol. 23, pp. 1–29).

Tappin, D. R. (2010). Submarine mass failures as tsunami sources: Their climate control. *Philosophical Transactions of the Royal Society a: Mathematical, Physical and Engineering Sciences, 368*(1919), 2417–2434. https://doi.org/10.1098/rsta.2010.0079

Tappin, D. R., Watts, P., McMurtry, G. M., Lafoy, Y., & Matsumoto, T. (2001). The Sissano, Papua New Guinea tsunami of July 1998—offshore evidence on the source mechanism. *Marine Geology, 175*(1–4), 1–23.

Titov, V. V. (2021). Hard lessons of the 2018 Indonesian tsunamis. *Pure and Applied Geophysics., 178*, 1121–1133. https://doi.org/10.1007/s00024-021-02731-0

Tsuji, Y., Matsutomi, H., Imamura, F., Takeo, M., Kawata, Y., Matsuyama, M., Takahashi, T., & Harjadi, P. (1995). Damage to coastal villages due to the 1992 Flores Island earthquake tsunami. *Pure and Applied Geophysics, 144*(3), 481–524. https://doi.org/10.1007/BF00874380

Twichell, D. C., Chaytor, J. D., ten Brink, U. S., & Buczkowski, B. (2009). Morphology of late Quaternary submarine landslides along the U.S. Atlantic continental margin. *Marine Geology, 264*(1), 4–15. https://doi.org/10.1016/j.margeo.2009.01.009

Vitousek, S., Barnard, P. L., Fletcher, C. H., Frazer, N., Erikson, L., & Storlazzi, C. D. (2017). Doubling of coastal flooding frequency within decades due to sea-level rise. *Scientific Reports, 7*, 1399. https://doi.org/10.1038/s41598-017-01362-7

von Huene, R., Kirby, S., Miller, J., & Dartnell, P. (2014). The destructive 1946 Unimak near-field tsunami: New evidence for a submarine slide source from reprocessed marine geophysical data. *Geophysical Research Letters, 41*, 6811–6818. https://doi.org/10.1002/2014GL061759

Ward, S. N. (1980). Relationships of tsunami generation and an earthquake source. *Journal of Physics of the Earth, 28*(5), 441–474. https://doi.org/10.4294/jpe1952.28.441

WorldPop (www.worldpop.org - School of Geography and Environmental Science, University of Southampton; Department of Geography and Geosciences, University of Louisville; Departement de Geographie, Universite de Namur) and Center for International Earth Science Information Network (CIESIN), Columbia University (2018). Global High Resolution Population Denominators Project - Funded by The Bill and Melinda Gates Foundation (OPP1134076). https://doi.org/10.5258/SOTON/WP00675

Ye, L., Kanamori, H., Rivera, L., Lay, T., Zhou, Y., Sianipar, D., & Satake, K. (2020). The 22 December 2018 tsunami from flank collapse of Anak Krakatau volcano during eruption. *Science Advances, 6*(3), eaaz1377. https://doi.org/10.1126/sciadv.aaz1377

Yeh, H., Imamura, F., Synolakis, C., Tsuji, Y., Liu, P., & Shi, S. (1993). The Flores Island tsunamis. *Eos, Transactions American Geophysical Union, 74*(33), 369–373. https://doi.org/10.1029/93EO00381

Yeh, H., Liu, P., Briggs, M., & Synolakis, C. (1994). Propagation and amplification of tsunamis at coastal boundaries. *Nature, 372*, 353–355. https://doi.org/10.1038/372353a0

Yue, H., Lay, T., Rivera, L., Bai, Y., Yamazaki, Y., Cheung, K. F., Hill, E. M., Sieh, K., Kongko, W., & Muhari, A. (2014). Rupture process of the 2010 M w 7.8 Mentawai tsunami earthquake from joint inversion of near-field hr-GPS and teleseismic body wave recordings constrained by tsunami observations: 2010 Mw 7.8 Mentawai tsunami earthquake. *Journal of Geophysical Research: Solid Earth, 119*(7), 5574–5593. https://doi.org/10.1002/2014JB011082

(Received August 25, 2021, revised April 28, 2022, accepted May 3, 2022, Published online May 30, 2022)